Journal of Applied Chemistry

Volume No. 11

Issue No. 1

January - April 2025

ENRICHED PUBLICATIONS PVT.LTD

JE - 18,Gupta Colony, Khirki Extn,
Malviya Nagar, New Delhi - 110017.
E- Mail: info@enrichedpublication.com
Phone :- +91-8877340707

Journal of Applied Chemistry

Aims and Scope

Journal of Applied Chemistry is a peer-reviewed, journal that publishes original research articles as well as review articles related to all aspects of applied chemistry. These includes the fields of analytical, inorganic, organic, physical and applied chemistry area. Review articles discussing specific areas of chemistry of current chemical importance are also published.

The journal welcomes publications of high quality papers on theoretical developments and practical applications in applied chemistry. Original research papers, state-of-the-art reviews, and high quality technical notes are invited for publications.

Journal of Applied Chemistry

Journal of Applied Chemistry

(Volume No. 11, Issue No. 1, January - April 2025)

Contents

Study on the Factors Influencing the Extraction of Chenodeoxycholic Acid from Duck Bile Paste by Calcium Salt Method

Xiangzheng Hu , Na Feng, and Jiaqi Zhang

College of Food Engineering & Biotechnology, Tianjin University of Science and Technology, Tianjin 300457, China

I. INTRODUCTION

Chenodeoxycholic acid (3**,**7**-dihydroxy-5**-cholanic acid,CDCA) is one of the dominant bile acids in human andanimals bile. CDCA has signifcant anti-infammatory, anti tussive, and expectorant efects [1]; CDCA is used for themedical treatment of metabolic diseases for it can reduce ordissolve cholesterol gall-stones in vivo [2]. CDCA is also theprecursor of ursodeoxycholic acid (UDCA) which is anotherefective drug for gallstone treatment [3, 4]. UDCA is usedto treat a variety of acute and chronic liver diseases [5–8].Te method of synthesizing of UDCA with CDCA is highlyefcient. Te cost of producing UDCA by this method is thelowest. At present, the UDCA is mainly produced by this method [9–11].

CDCA is the main organic ingredient in the bile of chick ens, ducks, geese, and other poultry. It can be obtained frompoultry bile by extracting technology [12] or synthesizingfrom cholic acid, dehydrocholic acid, and so on. Initially, thesynthesis of CDCA from CA is the main source of CDCA.

In Europe, chemical synthesis of CDCA with CA as raw material is the main source of CDCA. In the past 10 yearsin China, the extraction of CDCA from chicken bile was themain source of CDCA. Although the number of chickens andducks in China is very large, diferent techniques are requiredfor extracting CDCA from chicken bile and duck bile becausethere is a large diference in the composition of chicken andduck bile. Few literatures report on the method of extracting CDCA from duck bile.

A typical process for preparing CDCA is as follows: esterifying of saponifed bile acid, acetylating of bile acid ester, removal of intermediate product by using organic solvent, crystallizing of acetylated ester of CDCA, deprotecting, and crystallizing in organic solvent.Te entire process is complex, a large number of organic solvents (e.g., ethyl acetate, gasoline) are consumed, and the yield of the fnal product is low.

At present, in China, because of being used as a raw material for CDCA extraction, the price of chicken bile is high.

Te duck bile is treated as a waste by a slaughterhouse for the lack of related technology, even though the content of CDCA in chicken bile and duck bile is similar. In order to solve theenvironmental pollution problems of duck bile and make iteasy to store and transport, many slaughterhouses turn duckbile into gall ointment which can be used as a feed.Te content of CDCA in duck bile is over 25%. Moreover,extracting CDCA from duck bile can bring considerableeconomic benefts. Tis paper is aimed at designing an efcient way to fnd out the primary factors infuencing the yield of CDCA from duck bile paste. We speculate that this aim could be easily realized through the combination of an orthogonal experimental design method.

2. Materials and Methods

2.1. Materials. Duck bile paste was obtained from Xiayi Kangda Biochemical Raw Materials Co., Ltd. Anhydrous methanol (MeOH), hydrogen peroxide (H2O2), calcium chloride (CaCl2), sodium hydroxide (NaOH), glacial acetic acid, ethanol, chloroform (CHCl3), and ethyl acetate weresupplied by Tianjin Chemical Reagent Company (Tianjin,China), and all of them were of analytical grade; the standardsample of CDCA was from inspection bureau biological project of China.

2.2. Apparatus and Detection. FTS135-FTIR Spectrometer (Bio-Rad Instruments) was used to determine the infraredspectra, and the measurements were carried out by theKBr method. AVIII 600 NMR Spectrometer (Bruker A.G)was used to determine the nuclear magnetic spectrum.Te conditions were 23 C and 400.4 MHz, and TMS wasused as the internal standard. For high-performance liquidchromatograph (Agilent), the chromatographic column wasa Waters Symmetry C18 (4.6 mm × 150 mm, 5 m). Temobile phase was 0.2% formic acid-methanol (20 : 80, v/v)and fow rate was 1.0 mL/min. Te column temperaturewas maintained at 30 C. Te standard curve was used to determine the purity of the CDCA by HPLC [13–15].

2.3. Orthogonal Experimental Design [16]. Orthogonal experimental design is a popular method to deal with the test, including multiple factors and levels. It has been successfullyapplied to many felds for acquiring the optimum level group.Te key of this method is making an orthogonal designtable based on the reasonable and representative levels of theinvestigated factors. Tis method can help us to select therepresentative cases for lowering the number of test cases. Inthis work, the number of investigated factors is four and they have three levels; an or thogonal design table 9(34)is needed, reducing the number of test cases from 81 to 9.

2.4. Process. Afer the solution of duck bile paste in CH3OH was heated to 65 C with stirring for 1 h, the solution was cooled to the room temperature. Insoluble substance was fltered out.

Te 10% H2O2 solution was added to the fltrate with stirring. Afer 30 min, 20.0% (w/v) CaCl2 solution wasadded to the solution; the pH value was adjusted to 11 with5% (w/v) NaOH solution. Te mixture was stirred for 30 min;the precipitation was formed. Te precipitate was collectedby centrifugation and then was added to 60% glacial aceticacid. Te solution was heated and kept refux until all solidwas dissolved. A yellow transparent solution was got. Tisliquid was poured into water afer cooling, and the CDCAsolid was obtained by fltration. Finally, CDCA was purifedby recrystallizing in EtOH/CHCl3 mixed solution.Te resultsshow that the amount of H2O2, MeOH, glacial acetic acid, and CaCl2 added afects the extraction of CDCA in duck

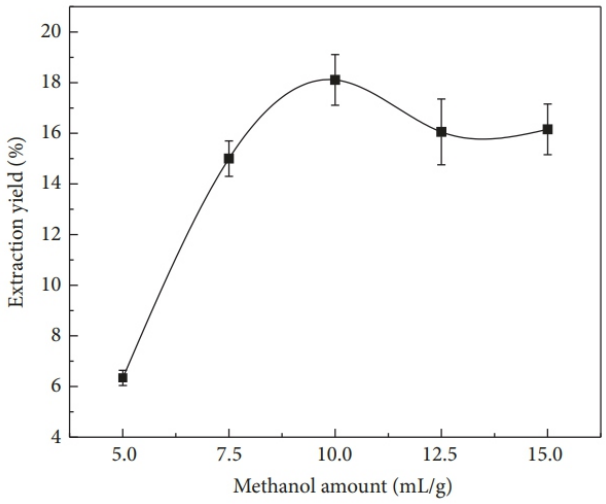

Figure 1: Efect of diferent amount of methanol on the yield of CDCA.

bile paste. Te single factor experiment conditions and orthogonal experiment conditions were determined based on the preliminary experimental results.

2.5. Calibration Curves. Te solutions were prepared by accurately weighing 50 mg CDCA standard and dissolving it in 50 mL methanol. Te working standard solution was prepared by diluting the mixed standard solution with MeOH to a series of proper concentrations. Te standard solutions were stored at 4 C until use.

Te sample solutions were prepared by accurately weighing 25 mg CDCA sample and dissolving it in 50 mL MeOH. Te resultant solution was fltered through a 0.45 m syringe flter (Type Millipore, USA); 20 L of the fltrate was injected into the HPLC system. Te sample solutions were stored at 4
C. Te working standard solutions were brought to room temperature and 50 L was injected into HPLC for the construction of calibration curves. A linear regression equation was obtained by plotting the logarithms of peak area responses versus logarithms of concentrations, in g/L.

3. Results and Discussion

3.1. Infuence of Diferent Amount of Reagent on Yield

3.1.1. Te Infuence of MeOH on Yield. Te duck bile pastes 100 g, 100 mL H2O2 solution, 300 mL 20.0% CaCl2 solution, and 600 mL 60% glacial acetic acid were added to the system.

Te infuence of MeOH on yield was shown in Figure 1.

When the amounts of H2O2, CaCl2, and glacial acetic acid were fxed, the yield of CDCA increased with the increasing amount of MeOH in a certain range. When the amount of MeOH reached about 1000 mL, the yield reached the maximum value. Afer that, with the dosage of MeOH kept increasing, the yield remained stable. Te results indicated that smaller amount of MeOH could not dissolve the paste completely. When the solvent was more enough, the yield

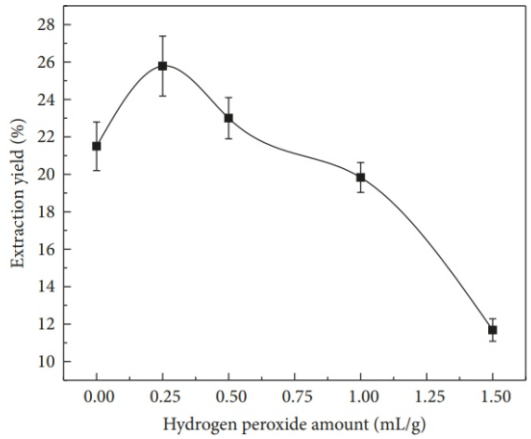

Figure 2: Efect of diferent amount of hydrogen peroxide on the yield of CDCA.

was not increased. So taking the cost of production into consideration, 1000 mL was suitable.

3.1.2.Te Infuence of H2O2 on Yield. Te duck bile paste 100 g was dissolved in the system composed of 1000 mL MeOH, 300 mL 20.0% CaCl2, and 600 mL 60% glacial acetic acid.Te impact of H2O2 amount on yield was shown in Figure 2.

When the amount of the H2O2 was added to 25 mL, the yield of CDCA reached the maximum value. Afer that the yield of CDCA decreased with the increasing of H2O2 solution. Tis situation may be as a result of the large amount of H2O2 oxidizing CDCA so as to reduce the yield of CDCA.

reached the maximum value when 400 mL CaCl2 solution was added.

When the amount of CaCl2 was not enough, the CDCA would not form CaCl2. On the contrary, if the amount was too large, it would generate Ca(OH)2, which could adsorb CaCl2 and decrease the yield of CDCA.

3.1.4. Te Infuence of Glacial Acetic Acid on Yield. Te duck bile paste 100 g was dissolved in 1000 mL MeOH, and then 100 mL H2O2 and 600 mL 20.0% CaCl2 solution were added with stirring. Te infuence of glacial acetic acid amount on yield was shown in Figure 4.

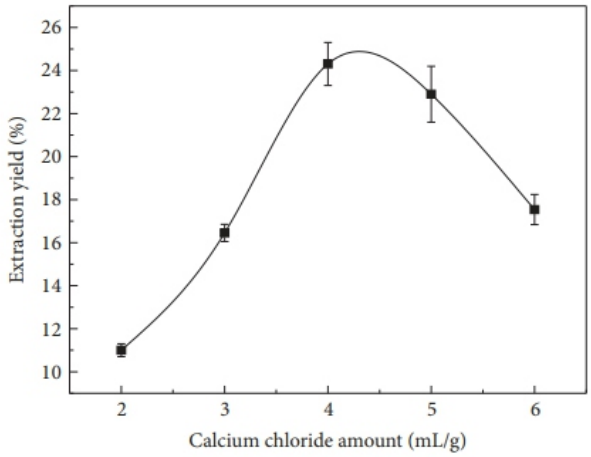

FIGURE 3: Effect of different amount of 20% calcium chloride on the yield of CDCA.

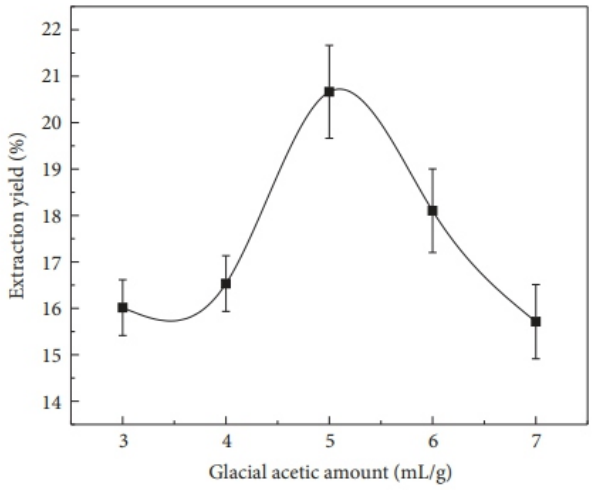

Figure 4: Efect of diferent amount of 60% glacial acetic acid on the yield of CDCA.

When the amount of glacial acetic acid added was less than 500 mL, the yield of CDCA increased with the increasing amount of glacial acetic acid. When the amount of glacial acetic acid added was 500 mL or more, the yield of CDCA decreased with the increase of glacial acetic acid amount. A small quantity of glacial acetic acid could neutralize calcium salt and lead to release of CDCA.

When the amount of glacial acetic acid reached 500 mL, the calcium salt of CDCA just hydrolyzed completely and the additive amount was suitable. While the amount of glacial acetic acid continuously is increased, CDCA would be dissolved, leading to yield decrease.

3.2. Orthogonal Test. Based on the above experimental data, taking the yield of CDCA as an index, orthogonal experimen tal design of four factors' three levels was taken to optimize the extracting conditions of CDCA. Te factors and levels are shown in Table 1. 9(34) orthogonal test results of intuitive

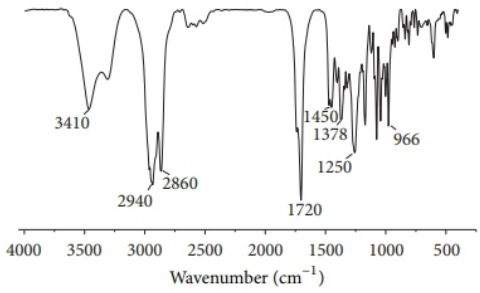

FIGURE 5: The IR of CDCA of sample product.

TABLE 1: Factors and levels for orthogonal test.

Level	A Methanol (mL)	B H_2O_2 (mL)	C $CaCl_2$ (mL)	D Glacial acetic acid (mL)
1	750	25	300	400
2	1000	50	400	500
3	1250	100	500	600

analysis were carried out as in Table 2. Variance analysis of orthogonal experiment results was shown in Table 3. Te analysis of variance was performed by statistical sofware SPSS 12.0.

Te results showed that factors infuencing the extraction of CDCA from duck bile paste by calcium salt were as follows:hydrogen peroxide, methyl alcohol, glacial acetic acid, andcalcium chloride. Te optimum extracting conditions of thisprocess were that every 100 g duck bile paste collocated with1000 mL MeOH, 50 mL H2O2, 500 mL 20% CaCl2 solution,and 600 mL 60% glacial acetic acid. A parallel experimentwas performed three times under the conditions of the bestcombination of factors; the yield was 30%, 29%, and 31%, andaverage value was 30%; it was signifcantly higher than singlefactor tests results.

3.3. Characterization

3.3.1. Structure Characterization

(1) IR Spectrogram. Te IR spectrogram of sample was shown in Figure 5.

In FTIR spectra, the appearance of a broad stretching vibration band at 3410 cm−1 for hydrogen groups and CH groups, C=O stretching vibrations, bend vibration for hydrogen groups, C-H bend vibrations, C-O in carboxyl groups at 2940, 1720, 1450, 1378, and 1250 cm−1 (close to the literature value [17]) determined that the obtained substance was CDCA.

(2) 1 ����. Te 1 HNMR spectrogram of sample was shown in Figure 6. 1 HNMR spectra were recorded in CDCl3 on a AVIII600 NMR Spectrometer (Bruker A.G), using TMS as internal

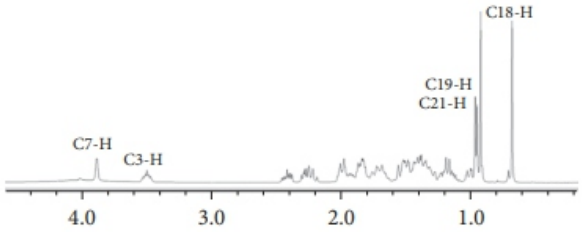

FIGURE 6: The HNMR spectrum of sample product.

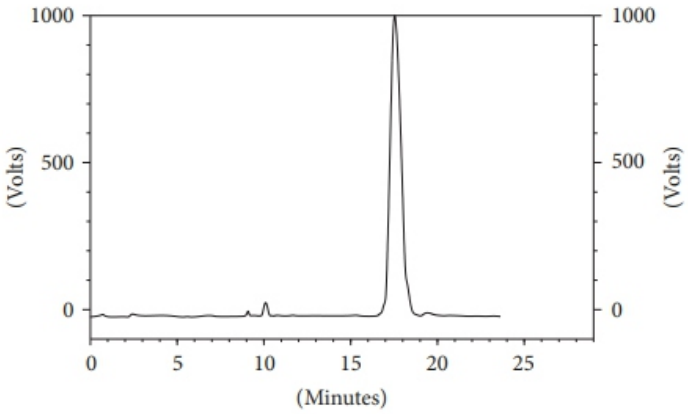

FIGURE 7: The HPLC spectrum of sample product.

standard. Figure 6 showed the characteristic peak value (�H 0.68 (s, 3H, 18-CH3), 0.92 (s, 3H, 19-CH3), 0.95 (d, 3H, 21- Ch3), 3.49 (br, 1H, 3-H), and 3.87 (br, 1H, 7-H)) (close to the literature value [18]). By the 1 HNMR spectrogram and the related literature [19], the obtained substance is determined to be CDCA.

3.3.2. Te Detection Results of HPLC. Te product was determined by HPLC. As shown in Figure 7, the retention time of CDCA was 17.3 min. Small impurity peaks can be seen at 10 min, and some of the corresponding materials were likely contained in the raw material. Te regression equation of CDCA was $\hat{} = 0.7229\hat{} + 16.908$ ($\hat{} = 0.9997$); CDCA in the 0.3 $\hat{}$g−0.7 $\hat{}$g/$\hat{}$L range showed a good linear relationship. According to the regression equation, the purity of CDCA was 97.2%.

4. Conclusions

Te detection data proved that the optimum extracting conditions were that every 100g duck bile paste collocated with 1000 mL MeOH, 50 mL H2O2, 500 mL of 20% CaCl2 solution, and 600 mL of 60% glacial acetic acid. Under the optimal extraction conditions, the yield of CDCA can reach 30%.

Over the years, CDCA is mainly obtained from chicken bile. In this paper, CDCA was extracted from the duck bile paste and the optimal extraction conditions were determined by orthogonal test. Te process is simple and suitable for industrial production, what is more, it can enhance the added value of livestock and poultry products.

Table 2: Analysis of $L_9(3^4)$ test results.

Test number	A	B	C	D	Productivity %
1	1	1	1	1	24
2	1	2	2	2	24
3	1	3	3	3	17
4	2	1	2	3	29
5	2	2	3	1	28
6	2	3	1	2	18
7	3	1	3	2	24
8	3	2	1	3	25
9	3	3	2	1	13
$K1$	65.20	76.81	66.53	64.92	
$K2$	74.83	77.12	66.1	65.61	
$K3$	60.89	46.99	68.29	70.39	
$k1$	21.73	25.60	22.18	21.64	
$k2$	24.94	25.71	22.03	21.87	
$k3$	20.30	15.66	22.76	23.46	
Range R	4.64	10.05	0.73	1.82	
Order	B > A > D > C				
Combination	$A_2B_2C_3D_3$				

Ki represents the sum of number i of various factors ($i = 1, 2, 3$), ki represents the average of number i of various factors ($i = 1, 2, 3$), R represents the difference between the maximum and the minimum of ki of various factors.

Table 3: Variance analysis of orthogonal experiment.

Factors	SS	f	F	F threshold	Significance
A	33.96	2	37.83	19	*
B	199.68	2	222.46	19	*
C	0.90	2	1	19	
D	5.92	2	6.59	19	
Error		2			

* indicates that this factor has significant influence on the experiment.

Conflicts of Interest

Te authors declare that they have no conficts of interest.

Acknowledgments

Tis work was supported by the Tianjin Science and Technology Project Funds (nos. 14ZXCXSY00109 and 14RCHZSY00159).

References

[1] R. A. Cao, L. Y. Li, and L. P. Zhang, "Study on the extractiontechnology of chenodeoxycholic acid from porcine bile," FoodResearch and Development, vol. 32, no. 4, pp. 12–15, 2011.

[2] A. F. Hofmann, "Bile acids: trying to understand their chemistryand biology with the hope of helping patients," Hepatology, vol.49, no. 5, pp. 1403–1418, 2009.

[3] J. Wan, J. He, and X. J. Cao, "A novel process for preparing purechenodeoxycholic acid from poultry bile," Journal of Industrialand Engineering Chemistry, vol. 18, no. 1, pp. 65–71, 2012.

[4] B. Alenezi, E. Lamoureux, L. Alpert, and A. Szilagyi, "Efectof ursodeoxycholic acid on granulomatous liver disease due tosarcoidosis," Digestive Diseases and Sciences, vol. 50, no. 1, pp.196–200, 2005.

[5] G. Paumgartner and U. Beuers, "Mechanisms of action andtherapeutic efcacy of ursodeoxycholic acid in cholestatic liverdisease," Clinics in Liver Disease, vol. 8, no. 1, pp. 67–81, 2004.

[6] G. H. Sauter, K. Tiessen, K. G. Parhofer, C. Jungst, S. Fischer, ¨and D. Jungst, "Efects of ursodeoxycholic acid on synthesis of ¨cholesterol and bile acids in healthy subjects," Digestion, vol. 70,no. 2, pp. 79–83, 2004.

[7] M. P. Guarino, S. Carotti, M. Sarzano et al., "Short-termursodeoxycholic acid treatment improves gallbladder bileturnover in gallstone patients: A randomized trial," Neurogastroenterology & Motility, vol. 17, no. 5, pp. 680–686, 2005.

[8] K. D. Lindor, K. V. Kowdley, E. J. Heathcote et al., "Ursodeoxy cholic acid for treatment of nonalcoholic steatohepatitis: resultsof a randomized trial," Hepatology, vol. 39, no. 3, pp. 770–778,2004.

[9] M. F. Lu, W. C. Yin, F. D. Wang, and D. M. Peng, "Improvedsynthesis of ursodeoxycholic acid," Chinese Journal of Pharmaceuticals, vol. 46, no. 10, pp. 1058-1059, 2015.

[10] H. M. Xu, "A process for preparing ursodeoxycholic acid,"CN104193792A,

[11] Y. X. Zhu, L. Jie, Y. Wu, and L. Hai, "Synthesis of a keyintermediate for ursodeoxycholic acid," Chemical Reagents, vol.34, no. 4, pp. 366–368, 2012.

[12] Y. H. Liu and X. Z. Hu, "Extraction technique of chenodeoxy cholic acid from duck bile paste," Journal of Tianjin Universityof Science & Technology, vol. 24, no. 3, pp. 43–45, 2004.

[13] Y. H. Yeh and D. F. Hwang, "High-performance liquid chro matographic determination for bile components in fsh, chickenand duck," Journal of Chromatography B: Biomedical Sciencesand Applications, vol. 751, article 1, 2001.

[14] B. Amplatz, E. Zohrer, C. Haas et al., "Bile acid prepara- ¨tion and comprehensive analysis by high performance liquidchromatography–high-resolution mass spectrometry," ClinicaChimica Acta, vol. 464, pp. 85–92, 2017.

[15] J. Kandrac, S. Kevresan, J. K. Gu, M. Mikov, J. P. Fawcett,and K. Kuhajda, "Isolation and determination of bile acids,"European Journal of Drug Metabolism and Pharmacokinetics,vol. 42, article 157, 2006.

[16] W. Zuo, E. Jiaqiang, X. L. Liu, Q. G. Peng, Y. W. Deng,and H. Zhu, "Orthogonal experimental design and fuzzy greyrelational analysis for emitter efciency of the micro-cylindricalcombustor with a step," Applied Termal Engineering, vol. 103,pp. 945–951, 2016.

[17] X. J. Pan and X. M. Zhang, "A new process for isolation andpurifcation of chenodeoxycholic acid from pig's bile paste,"Hebei Medical Journal, vol. 28, no. 2, pp. 147-148, 2006.

[18] Q. H. Deng, Y. Yao, T. Liu, L. L. Jing, and Z. C. Li, "Te extractionand purifcation of three kinds of bile acids from pig bile,"Chinese Journal of Biochemical Pharmaceutics, vol. 33, no. 4, pp.405–407, 2012.

[19] D. V. Waterhous, S. Barnes, and D. D. Muccio, "Nuclearmagnetic resonance spectroscopy of bile acids. Development oftwo-dimensional NMR methods for the elucidation of protonresonance assignments for fve common hydroxylated bileacids, and their parent bile acid, 5 beta-cholanoic acid," TeJournal of Lipid Research, vol. 26, article 1068, 1985.

Phosphorus Speciation by 31P NMR Spectroscopy in Leaf Litters and Crop Residues from Para Rubber, Cocoa, Oil Palm, and Banana Plantations in the Humid Forest Zone of Cameroon

Lawrence Tatanah Nanganoa and Jetro Nkengafac Njukeng
Institute of Agricultural Research for Development (IRAD), Ekona Regional Centre, PMB 25, Buea, Southwest Region, Cameroon

A B S T R A C T

Te release of nutrients, including phosphorus from agricultural residues, is an important potential source of nutrients for subsequent crops. To fully understand the contribution of this residue P as a source of plant P for agricultural production, itschemical nature needs to be understood. In this study P species were identifed and quantifed in leaf litters and crops residuesfrom cocoa farms, oil palm, rubber, and banana plantations by 31P nuclear magnetic resonance (NMR) spectroscopy. Phosphorusin the crop residues was predominantly in the form of inorganic P mainly as orthophosphate and ranged from 45.9 to 89.2%. Tehighest relative percentage of P as orthophosphate was found in cocoa pod husk (89.2%) and the lowest percentage was found indecaying banana pseudostem (45.9%). Pyrophosphate was detected in trace amounts in all samples (less than 6%) except in freshpalm fronds. However, orthophosphate diester was detected only in fresh palm fronds (11.4%) and phytate was detected only inpalm male inforescence (6.7%). Te result implied that cocoa pod husk, palm empty fruit bunch, and palm male inforescencecould be used as organic amendment, based on their high P content and release potential

INTRODUCTION

Phosphorus defciency in many tropical soils is a major constraint of crop production. Tis defciency is primarily asa result of inherent low soil P, depletion of soil P by cropping,and sorption and precipitation involving Fe and Al oxidesand hydroxides [1]. Phosphorus is a major plant nutrientwhich is involved in many metabolic processes [2]. It is of enreferred to as “energizer” since it helps to store and transferenergy during the process of photosynthesis. According toFrossard et al. [3] only a small proportion of P in soil isfound in the soil solution (e.g., 0.01–3.0 mg P L−1) or in formsavailable to crop plants at any given time. Tus to improvecrop production, most farmers have depended on the useof P fertilisers. Te release of nutrients, including P fromlitters and crop residues, is an important potential source ofnutrients for subsequent crops [4, 5]. Total P in plant materialranges between 0.5 and 10 g kg−1. Inorganic orthophosphate,which is the preferred source of P to plants, is also themajor form of P found in green crops (60–80% of total P)during vegetative growth [3, 6, 7]. At physiological maturity,nutrients in crop residues can be released to the soil wherethey are incorporated into diferent labile and nonlabile pools[8]. For example, Seephueak et al. [9]

showed that in the para rubber plantation ecosystem, leaf litter is a major contributor to nutrient cycling pathways. Studies by Khalid et al. [10] showed that oil palm residues during replanting contributed signifcant amount of nutrients that could be recycled in the plantation. According to Hartemink [11] rain wash and litter fall are key components in the cycling of nutrients of cocoa ecosystems. Wortman et al. [12] also demonstrated that the management of harvested (senescent) banana pseudostem was found to be very important in the nutrient use efciency of banana plantations with most of their nutrients translo cated to the attached growing pseudostems.

Te major gap in soil fertility recommendations for the tropics is phosphorus management as crop production on many of the soils in the tropics is limited primarily by phosphorus.Te understanding of soil phosphorus dynamics and indicators of phosphorus availability lags far behind that

Land use type	Location	Longitude	Latitude	Elevation (m)	Soil type
Banana	Mussaka	04° 11.468′	009° 19.25′	477	Volcanic soil
Cocoa	Ekona	04° 06.167′	009° 23.51′	34	Volcanic soil
Rubber	Misellele	04° 07.555′	009° 26.62′	35	Volcanic soil
Oil palm	Maumu	04° 12.29′	009° 19.76′	437	Volcanic soil

for nitrogen. Part of the problem in modelling phosphorus is in its complex biogeochemical cycle [13]. Optimizing P use efciency is very important for agronomic, economic,and environmental benefts especially when adjusting agricultural production systems to meet future global foodproduction targets [14]. Such optimization will rely onadequate knowledge of the dynamics of soil and residueP pools to enable accurate predictions of the requiredexternal P inputs to achieve optimum growth of subsequent crops.

Te most commonly used measure of P in crop residues is total P, followed by the distinction between inorganic Pand organic P. Te carbon : phosphorus (C : P) ratio of cropresidues has ofen been widely used to predict potentialP immobilization or mineralization [15]. However, thesemeasures do not identify or take into account the various Pspecies found within crop residues. Te employment of 13PNMR spectroscopy has greatly improved the understandingof soil P species, particularly the organic P forms quantifedin relative terms [16]. P speciation is also important forthe estimation of P release from crop litters and residuesin cropping soils, as some species of P in residues maybe more recalcitrant than others. Few studies have usedsolution NMR to identify P species in fresh and matureplant materials and mature crop residues [8]. However, thistechnique has not been used to identify P forms in littersand residues of para rubber, cocoa, oil palm, and bananaplantations. Phosphorus in soil is generally divided intoorganic P and inorganic P [17, 18].

Inorganic P is classifed into orthophosphate, pyrophosphate, and polyphosphate.Typical organic P compounds are divided into phosphatemonoesters, phosphate diesters, phosphonates, and organicpolyphosphates. However, knowledge of how these P formschange as plants senesce is limited, since most research inthis area focused on fresh or immature plant materials ratherthan the senesced materials that are returned to soil in mostfarming systems [19]. To fully understand the contributionof crop residue P as a source of plant P for agriculturalproduction, its chemical nature needs to be understood. Tisis a prerequisite to further understand the dynamics of cropresidue P in the soil ecosystem, and its bioavailability to plantsand microorganisms. Proper identifcation of P species incrop litters and residues can improve the understanding ofthe potential turnover of these P species in soil, leading to abetter assessment of the amount of P that may be provided for subsequent crops.

Te objective of this study therefore is to identify and quantify the various phosphorus species in leaf litters andcrop residues from cocoa farms, oil palm, rubber, and bananaplantations.

Table 2: Samples used and code names.

Sample name	Description
JN-01	Cocoa pod husk
JN-02	Senescent cocoa leaves (litter)
JN-03	Fresh banana pseudostem
JN-04	Decaying banana pseudostem
JN-05	Fresh palm fronds
JN-06	Palm empty fruit bunches
JN-07	Palm male inflorescence
JN-08	Senescent rubber leaves (litter)

2. Materials and Methods

2.1. Site Description. Samples were collected from some banana, cocoa, rubber, and oil palm felds in Fako Division of the South West region of Cameroon. Te banana, rubber, and oil palm felds belong to the Cameroon Development Cooperation (CDC) and the cocoa farm to a small holder farmer. Te exact locations of the felds are presented in Table 1.

Te study area (Fako division) has humid tropical cli matic conditions and rich volcanic soils with two distinctive seasons, a long rainy season which ranges from midMarch to mid-November and a short four-month dry season expanding from mid-November to mid-March [21, 22]. In cocoa farms the main source of organic waste is the cocoa pod husk which is lef in the felds afer bean harvest. Tere are ofen in large quantities because for a cocoa pod, just 30% of its weight is made up of the cocoa bean and the rest is the husk. Another source of organic waste in cocoa farms is the leaf litter (senescent leaves).

In mature oil palm plantations in Cameroon the fronds (branches) are ofen cut and lef torot in the felds which is the main source of organic waste.Te empty fruit bunches and the male inforescence is alsoresidues of the oil palm plantation. In rubber plantationsthere is the annual leaf fall referred to as defoliation wherethe rubber tree shades all its leaves and this forms the mainsource of organic waste (leaf litter) in rubber plantations. Inbanana plantations, the main organic waste is the stems that remain afer bunch harvest.

2.2. Sample Collection. For each agroecosystem, the main organic wastes were identifed and samples of about 10 kgcollected. Te samples were sun dried to reduce the moisturecontent and reduce the risk of molds growing on the samples.Te dried samples were ground into powder and packagedin polyethylene bags for analyses. Table 2 shows the sample codes and their description. Tese agricultural crop residues

Table 3: Some physical properties of the samples, pH, organic matter (%), moisture, ash (%), and organic carbon content.

Sample	pH(H_2O)	Moisture content (%)	Organic matter (%)	Ash content (%)	[a]Organic carbon (%)
JN-01	8.17	10.2	91.7	8.3	53.3
JN-02	6.52	5.3	85.7	14.4	49.8
JN-03	9.28	4.9	80.9	19.1	47.0
JN-04	10.29	7.4	68.8	31.2	40.0
JN-05	5.82	5.2	91.2	8.8	53.0
JN-06	7.55	5.1	93.3	6.8	54.2
JN-07	7.58	14.0	88.0	12.1	51.1
JN-08	6.75	6.00	94.5	5.5	55.0

[a]Estimated by a conversion factor of 1.72.

were distinguished into feld residues (JN-02, JN-03, JN04, JN-05, JN-07, and JN-08), which are materials lef in an agricultural feld afer the crop has been harvested, and process residues (JN-01 and JN-06), which are materials lef afer the crop is processed into a usable resource.

All the crop residue samples were analyzed for pH, organic matter, ash content, moisture content, and P species.

2.3. Physicochemical Analysis of Crop Residues and Leaf Litters.

Te pH was measured in H2O (ratio soil : water 1 : 2.5 w/v).

Percentage of ash content and organic matter (OM) was determined by loss of ignition using 0.5 g of sample heated up to 550 C in a mufe furnace (Carbolite, UK) for 4 hours.

Total P was determined in samples using a nitric acid (HNO3) digestion method. 0.5 g of plant material was digested with 5 mL of HNO3 (Sigma Aldrich reagent grade, 69%) for up to 4 hours. Phosphorus concentration in all digests was measured by Colorimetry [20].

2.4. Solution 31P: NMR Spectroscopy Analysis

2.4.1. NaOH-EDTA Extraction. Te sample preparation for solution 31P NMR spectroscopy was performed using a modifed procedure as described in Ebuele et al. [23]. 1 g of crushed freeze-dried crop residue sample was mixed with 25 mL of a solution of 0.25 M NaOH and 0.05 M EDTA and shaken at 250 rpm at 20 C for 6 hours. Te extracts were then centrifuged for 20 minutes at 5000 rpm and fltered using Whatman number 42 flter paper. An aliquot of 0.5 mL was then diluted for colorimetric analysis and the remaining solution was freeze-dried.

Approximately, 100 mg of each freeze-dried extract was redissolved in 0.6 mL of D2O, 0.5 mL 10 M NaOH, and 0.4 mL extracting solution (0.25 M NaOH + 0.05 M EDTA).
Samples were centrifuged for 60 minutes at 2500 (to remove particles that might contribute to line broadening) and then transferred to a 5 mm NMR tube and analyzed via 31P NMR spectroscopy.

2.4.2. Identifcation and Quantifcation of Phosphorus Species Using 31P NMR. Spectra were acquired on a Bruker Avance DRX 400 MHz NMR spectrometer (7.5 T, 161.9 Mhz), equipped with a 5 mm broadband probe at 20 C. Instrument parameters were a 90 pulse, 0.68 s acquisition time, and recovery delay of 4.32 s to 15 s. Inverse gated proton decoupling was used and set to at least fve times the 1 (lattice relaxation time). In the experiment, between 3000 scans to 5000 scans (4–7 hours of running time)were required to achieve a good signal to noise ratio. Tespectral width used was 8090.6 Hz and the number ofdata points was 11002. Te chemical shif (ppm) of thesignals was indirectly referenced to an external 85% H3PO4standard via the lock signal. Peaks were defned by threeparameters: chemical shif, line width, and peak height.Peak assignment was based on literature data [8, 24–27].Integration of peak areas was calculated on spectra processedwith a line broadening of 1–10 Hz using a Bruker Topspin2.0 sofware and MestReNova v.7.0. Quantifcation of Pspecies was done by spectra deconvolution analysis basedon the chemical shif, peak width, and peak area, whichproved to be successful in particular for areas such as themonoester region containing a number of peaks, sometimesoverlapping; the relative P concentration in the NaOH-EDTAextracts was estimated, based on the total NMR signal area,and presented as percentages of each specie or group ofspecies.

3. Results and Discussions

3.1. Physicochemical Properties of Crop Residues and Leaf Litters. A summary of some physicochemical propertiesof the samples is presented in Table 3. Te characteristicsof the plant residues vary which is due to diferences inplant species, plant tissues, and soil chemical and physicalproperties [28].

Te crop residues and leaf litters exhibited a wide range of pH (5.82–10.29). Tis can be categorized into 4 groups: weakly acid (JN-02, JN-05), neutral (JN-06, JN-08, JN-07), weakly basic (JN-01, JN-03), and basic (JN04). Te palm male inforescence (JN-07) had the highest moisture content (14.0%) as compared to the other plant residues. Te plant residues had relatively high ash content ranging from 5.5% (JN-08) to 31.2% (JN-04). Tese high ash content values can be attributed to the incorporation of inorganic materials in the residues [29]. On the other hand the samples were quite high in organic matter (85–94.5%) except for the decaying banana pseudostem which was low and this could account for its highest value of ash (31%).Tese high levels of organic matter is in agreement with the study of Naklang et al., [30] who concluded that crop residues,

Table 4: Te relative percentage of total extractable inorganic and organic P species in the NaOH-EDTA extracts based on total NMR peak area. Total P and total NaOH -EDTA-P concentration in mg kg−1 and % recovery.

Samples	Inorganic P		Organic P			[a]Total P (HNO_3) mg kg^{-1}	[a]Total NaOH-EDTA-P mg kg^{-1}	Recovery %
	Ortho-P	Pyro-P	Phytate	Other monoesters	Other diesters			
	Relative percentage (%)							
JN-01	89.2	5.8	-	5.0	-	1436.0	1113.4	77.5
JN-02	79.6	4.6	-	15.9	-	729.8	688.4	94.3
JN-03	72.5	3.1	-	24.4	-	1252.1	1112.9	88.9
JN-04	45.9	14.3	-	39.9	-	986.1	821.9	83.4
JN-05	54.3	-	-	34.3	11.4	1221.9	968.9	79.3
JN-06	81.4	4.8	-	13.8	-	1449.4	1260.8	87.0
JN-07	85.5	2.6	6.7	5.1	-	4001.2	4229.8	105.7
JN-08	53.0	5.7	-	41.3	-	865.2	618.9	71.5

[a]Determined by Colorimetry [20].

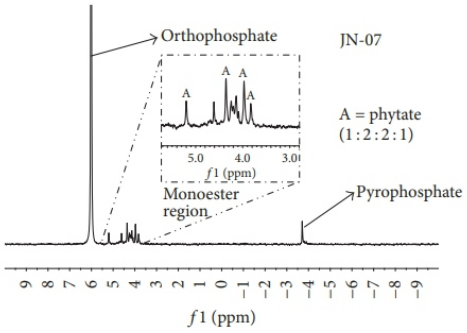

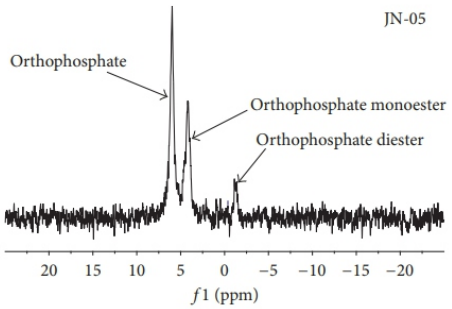

Figure 1: Solution 31P NMR spectra of crop residue extracts (JN-07) showing orthophosphate, pyrophosphate, orthophosphate monoesters, and diesters. Te inset shows the orthophosphate monoester region including peaks for phytate (A). leaf litters, and green manures are needed to rehabilitate soil carbon.

3.2. Phosphorus Species in NaOH-EDTA Extracts. Figure 1 shows the 31P NMR spectra of the various P species found in the NaOH- EDTA crop residue extracts using JN-07 as an example. All samples showed a peak between 5.88 and 6.05 ppm, characteristic resonances for orthophosphate (Figures 1, 2, and 3). Te other inorganic P species detected was pyrophosphate between −3.5 and −3.8 ppm, identifed in all samples except JN-05 (Figure 2).Te organic orthophosphate monoesters showed resonances from 3.8 to 5.2 ppm (Figure 1, inset) and the only diester P compound was detected in sample JN-05 (Figure 2) at −1.15 ppm at a very low resonance intensity and was attributed to nonhydrolyzed DNA [31, 32].

Phytate (Myo-Inositol hexakisphosphate) was identifed at 5.2, 4.4, 4.0, and 3.8 ppm (Figure 1, inset peak A) with the signals occurring in a ratio of 1 : 2 : 2 : 1, corresponding to the phosphate ion group on the inositol ring confrming the phytate peak [31]. Other resonances in the monoester region, occurring between 3.8 and 5.2 ppm, were attributed JN-05 Orthophosphate diester Orthophosphate monoester Orthophosphate f1 (ppm) 20 15 10 5 0 −5 −10 −15 −20
Figure 2: A solution 31P NMR spectrum of crop residue extracts (JN-05) showing orthophosphate diesters.to lower inositol phosphates, sugar phosphates, mononu cleotides, and phospholipid degradation products ﬂ- and ﬂ- glycerophosphate. Sample JN-07 is male palm inforescence and its highest phytate is similar to observations by Mitchell and Allsopp [33] who found phytate to be the main P species in seeds of Hakea sericea. Te highest value of phytate P also agrees with the work of Reddy et al., [34] who confrmed that the majority of P stored in plant seed is in the form of phytate.

3.3. Phosphorus Species Quantifcation. Te concentration of total P (Nitric acid digestion) and extractable NaOHEDTA in the crop residue extracts is shown in Table 4.

Extraction efciency (or recovery%) ranged from 72 to 105%, with sample JN-08 giving the lowest extraction efciency compared to other samples. In general, the results showed a high extraction efciency which means that there is little P in the leaf litters and crop residues that were not included in the NMR analysis. Te relative percentages of P species found in the NaOH-EDTA extracts are also listed in Table 4.

31P NMR spectra showed the presence of orthophosphate, pyrophosphate, phosphate monoesters, and diesters, while phosphonates and polyphosphates were not detected in any of the NaOH-EDTA crop residue extracts (Figures 1, 2, and 3). Phosphorus in the crop residues was predominantly in

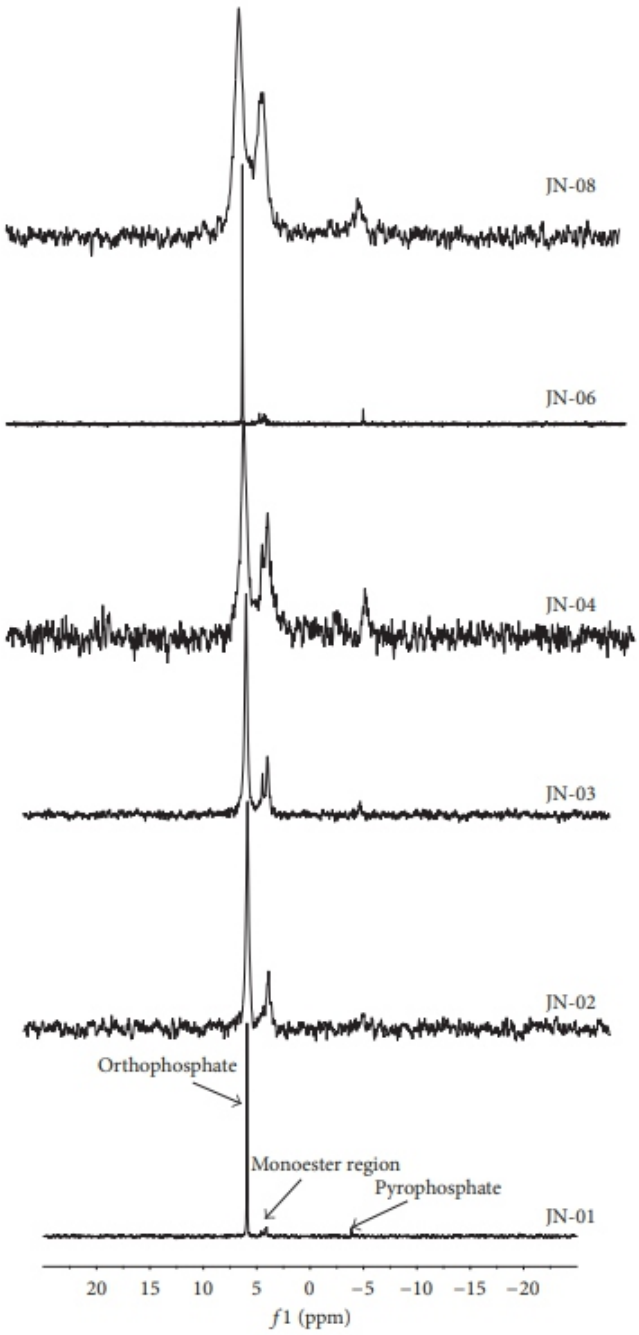

Figure 3: Solution 31P NMR spectra of NaOH-EDTA leaf litters and crop residue extracts for JN-01, JN-02, JN-03, JN-04, and JN-06, JN08.

the form of inorganic P mainly as orthophosphate and ranges from 45.9 to 89.2% with respect to total NaOH- EDTA extractable P (Table 4). Tis agrees with the results of Noack et al., [8] who reported that a very high proportion of P in crop residues exists as orthophosphate. Tis orthophosphate in the residues has the potential to be returned to the soil in a readily available form for plants (via root uptake) and microorganisms, as well as sorption onto soil minerals. Te highest relative percentage of P as orthophosphate was found

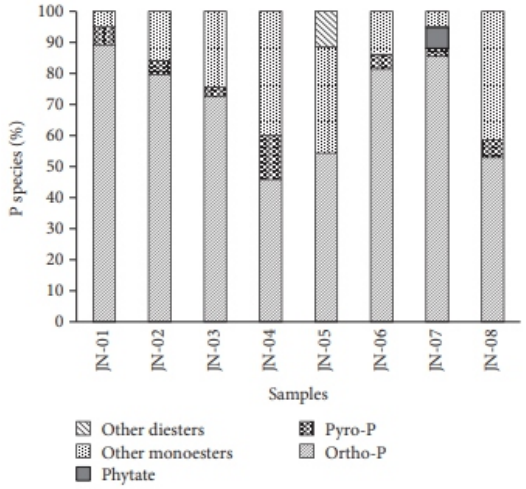

FIGURE 4: Relative percentages of P species in the crop residues.

in sample JN-01 (89.2% of total NaOH-EDTA extractable P) and the lowest percentage was found in sample JN-04 (45.9%of total NaOH-EDTA extractable P). Sample JN-01 is cocoapod husk and the results of this study are in agreement withthose of Adejobi et al., [35] who found high concentrationsof P in cocoa pod husk. Te other major inorganic Pspecies, pyrophosphate, was detected, in all samples exceptJN-05. Pyrophosphate was detected in trace amounts in allother samples (less than 6%) but was unusually high insample JN-04 (14.2% of total NaOH-EDTA extractable P).Pyrophosphate is the simplest inorganic polyphosphate andis essential for cellular functioning of living organisms [8]and it absence in fresh palm fronds (JN-05) suggests thatits availability may be governed by chlorophyll content. Tesecond most abundant P species were the organic P formsmainly as orthophosphate monoesters. Organic P speciationvaried across crop residue types. Te highest percentageof orthophosphate monoesters was found in sample JN-08(41.3% related to total NaOH-EDTA extractable P), whilethe lowest was in sample JN-01 (4.9% of total NaOH EDTA extractable P). Phytate (myo-inositol phosphate) wasdetected in only sample JN-07 (6.7% of total NaOH-EDTAextractable P) (Table 4, Figure 1). Te results of Table 4 alsoshowed that total P was very high for JN-07 as compared to the other crop residue samples.

Other organic P species detected in the samples would likely include degradation products such as -and -glycerophosphate (most likely originated from phospholipidusually found in plants) and mononucleotides (likely fromnucleic material found in plant cells), group under othermonoesters (Figure 4 and Table 4). Te only orthophosphatediester detected was in sample JN-05 (11.4% of total NaOHEDTA extractable P).Overall, the P species detected in all the crop residueswere similar for all the diferent samples and in line withpreviously reported P forms in other plant based crop

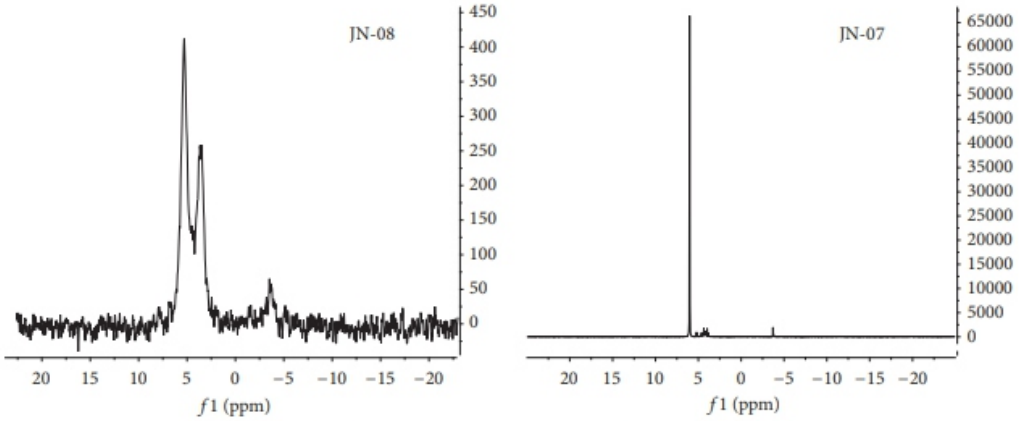

FIGURE 5: Comparison between the peak intensities of samples JN-07 and JN-08.

residues [8, 25, 27, 32]. Te poor resolution shown by feld residues samples (JN-02, JN-03, JN-04, JN-05, and JN-08)with the exception of JN-07 was evident in their relativelylower peak intensities, compared to process residues samples(JN-01 and JN-06) (Figure 5 for clarity). Te higher intensities shown by samples JN-01, JN-06, and JN-7 alsosuggest that they would likely contain higher concentrationsof P compared to the other samples; this was also supported by the elemental P data in Table 4.

Te other inorganic P form detected pyrophosphates are the smallest group of inorganic condensed polyphosphates,found in nature. Tey have also been found in plant tissuessuch as stems [8]. Teir main functions in plants includeacting as a storage form of P when inorganic P is in excess,and as a sink or strong chelator of metals ions such as Ca2+,Mn2+, and Mg2+ [36]. Phytate detected only in sample JN-07has been reported to be very stable under alkaline solutionsand is also one of the primary storage forms of P in plants(most especially in seeds). Te absence of stable diesterssuch as DNA in most of the 31P NMR spectra was likelyas a result of their low concentration and signals to noiseratio, making them relatively unquantifable. However, thelow concentration or complete absence of these diesters Pcompounds in the analyzed crop residue extracts can also belikely governed by their relative instability in NaOH-EDTAalkaline solution. Tis suggest that the higher percentages ofmonoesters relative to diesters detected in the crop residueextracts either are present in the samples or are degradationproducts of alkaline hydrolysis [37, 38]. Tis usually occursduring the extraction and redissolving processes required for31P NMR, thereby leading to an underestimation of diesters and overestimation of monoesters.

4. Conclusion

Eight crop residue samples were analyzed for P species using 31P NMR spectroscopy to quantify the various P forms inthe materials. Te crop residues were distinguished as feldresidues (JN-02, JN-03, JN-04, JN-05, JN-07, JN-08) andprocess residues (JN-01 and JN-06). Based on P speciationdata obtained, the recommended crop residues that shouldbe used as phosphorus sources were samples JN-01, JN-06,and JN-07 (i.e., cocoa pod husk, palm empty fruit bunch,and palm male inforescence). Te results demonstrated thatphosphorus in the crop residues was predominantly in theform of inorganic P mainly as orthophosphate which is aform readily available for plants uptake and microorganisms,as well as sorption onto soil minerals. Te orthophosphatemonoesters were the second major P group detected inall samples, with phytate detected only in sample JN-07.Orthophosphate diesters were detected in only one sample(JN-05), while pyrophosphate was detected in all samples except JN-05.Te result also suggested that sample JN-07 was likely from a seed based plant. Tis study shows that feldresidues especially male inforescence should be allowed torot in the feld.Te process residues should be thrown back tothe feld to rot or composted as these materials are important sources of P.

Conflicts of Interest

Te authors declare that there are no conficts of interest regarding the publication of this paper.

Acknowledgments

Sample analyses and data evaluation were undertaken by Victor Ebuele and Vera Fitzsimmons-Toss. Dr. VeraFitzsimmons-Toss is also acknowledged for allowing the useof her lab and for support with consumables, while the Schoolof Chemistry Bangor University Wales, United Kingdom,is acknowledged for the use of the NMR and general lab equipment.

References

[1] D. Solomon and J. Lehmann, "Loss of phosphorus from soil in semi-arid northern Tanzania as a result of cropping: evidence from sequential extraction and 31P-NMR spectroscopy," Euro pean Journal of Soil Science, vol. 51, no. 4, pp. 699–708, 20

[2] N. O. Nelson and R. R. Janke, "Phosphorus Sources Management in Organic Production Systems," Hortechnology,vol. 17, no. 4, pp. 442–454, 2007.

[3] E. Frossard, L. M. Condron, A. Oberson, S. Sinaj, and J.C. Fardeau, "Processes governing phosphorus availability intemperate soils," Journal of Environmental Quality, vol. 29, no.1, pp. 15–23, 2000.

[4] G. J. Blairk and O. W. Boland, "Te release of phosphorus fromplant material added to soil," Australian Journal of Soil Research,vol. 16, no. 1, pp. 101–111, 1978.

[5] M. J. McLaughlin, A. M. Alston, and J. K. Martirio, "Phosphorus cycling in wheat-pasture rotations. iii.organic phosphorus turnover and phosphorus cycling," Australian Journal of SoilResearch, vol. 26, no. 2, pp. 343–353, 1988.

[6] R. E. White and A. T. Ayoub, "Decomposition of plant residuesof variable C/P ratio and the efect on soil phosphate availability," Plant and Soil, vol. 74, no. 2, pp. 163–173, 1983.

[7] P. Hinsinger, "Bioavailability of soil inorganic P in the rhizo sphere as afected by root-induced chemical changes: a review,"Plant and Soil, vol. 237, no. 2, pp. 173–195, 2001.

[8] S. R. Noack, M. J. McLaughlin, R. J. Smernik, T. M. McBeath,and R. D. Armstrong, "Crop residue phosphorus: Speciationand potential bio-availability," Plant and Soil, vol. 359, no. 1-2,pp. 375–385, 2012.

[9] P. Seephueak, V. Petcharat, and S. Phongpaichit, "Fungi asso ciated with leaf litter of para rubber (Hevea brasiliensis),"Mycology, vol. 1, no. 4, pp. 213–227, 2010.

[10] H. Khalid, Z. Z. Zin, and J. M. Anderson, "Nutrient cyclingin an oil palm plantation: Te efects of residue managementpractices during replanting on dry matter and nutrient uptakeof young palms," Journal of Oil Palm Research, vol. 12, no. 2, pp.29–37, 2000.

[11] A. E. Hartemink, "Nutrient Stocks, Nutrient Cycling, andSoil Changes in Cocoa Ecosystems: A Review," Advances inAgronomy, vol. 86, pp. 227–253, 2005.

[12] C. Wortman, E. Karamura, and C. Gold, "Nutrient fows fromharvested banana pseudostems," African Crop Science Journal,vol. 2, no. 2, pp. 179–182, 1994.

[13] "Modelling nutrient management in tropical cropping systems,"in ACIAR Proceedings, R. J. Delve and M. E. Probert, Eds., 114,138 pages, 2004.

[14] P. Hefer and M. Prud'homme, "Nutrients as limited resources:global trends in fertilizer production and use," in ImprovingWater and Nutrient-use Efciency in Food Production Systems,Z. Rengel, Ed., pp. 57–78, John Wiley & Sons, 2013.

[15] A. B. Kwabiah, C. A. Palm, N. C. Stoskopf, and R. P. Voroney,"Response of soil microbial biomass dynamics to quality ofplant materials with emphasis on P availability," Soil Biology &Biochemistry, vol. 35, no. 2, pp. 207–216, 2003.

[16] B. Zhou, R. D. Vogt, X. Lu et al., "Land use as an explanatory factor for potential phosphorus loss risk, assessed by P indices andtheir governing parameters," Environmental Science: Processes &Impacts, vol. 17, no. 8, pp. 1443–1454, 2015.

[17] L. M. Condron, B. L. Turner, and B. J. Cade-Menun, "Chemistryand Dynamics of Soil Organic Phosphorus," in Phosphorus:Agriculture and the Environment, J. T. Sims and A. N. Sharpley,Eds., Agron. Monogr. 46. ASA, CSSA, and SSSA, pp. 87–121,Madison, WI, 2005.

[18] G. M. Pierzynski, R. W. McDowell, and J. T. Sims, "Chemistry, Cycling And Potential Movement of Inorganic Phosphorus inSoils," in Phosphorus: Agriculture and the environment, J. T. Simsand A. N. Sharpley, Eds., Agron. Monogr. 46. ASA, CSSA, andSSSA, pp. 53–86, Madison, WI, 2005.

[19] S. R. Noack, Crop Residue Phosphorus: Speciation and Release inCropping Soils. Doctor of Philosophy Tesis, School of Agriculture, Food and Wine, University of Adelaide, Australia, 2014.

[20] J. Murphy and J. P. Riley, "A modifed single solution methodfor the determination of phosphate in natural waters," AnalyticaChimica Acta, vol. 27, pp. 31–36, 1962.

[21] N. B. Sounders, T. E. Sunjo, and M. F. Mbella, "Efects of Rainfalland Temperature Oscillations on Maize Yields in Buea SubDivision, Cameroon," Journal of Agricultural Science, vol. 9, no.2, pp. 63–72, 2017.

[22] V. E. Manga, C. M. Agyingi, and C. E. Suh, "Trace Element SoilQuality Status of Mt. Cameroon Soils," Advances in Geology, vol.2014, Article ID 894103, 8 pages, 2014.

[23] V. O. Ebuele, A. Santoro, and V. Toss, "Characterization ofPlant Seeds by Phosphorus-31 Nuclear Magnetic ResonanceSpectroscopy," Analytical Letters, vol. 50, no. 6, pp. 999–1012,2017.

[24] B. L. Turner and A. E. Richardson, "Identifcation of scyllo inositol phosphates in soil by solution phosphorus-31 nuclearmagnetic resonance spectroscopy," Soil Science Society of Amer ica Journal, vol. 68, no. 3, pp. 802–808, 2004.

[25] M. I. Makarov, L. Haumaier, and W. Zech, "Te nature andorigins of diester phosphates in soils: A 31P-NMR study," Biologyand Fertility of Soils, vol. 35, no. 2, pp. 136–146, 2002.

[26] R. J. Smernik and W. J. Dougherty, "Identifcation of phytate inphosphorus-31 nuclear magnetic resonance spectra: Te needfor spiking," Soil Science Society of America Journal, vol. 71, no.3, pp. 1045–1050, 2007.

[27] S. R. Noack, M. J. McLaughlin, R. J. Smernik, T. M. McBeath,and R. D. Armstrong, "Phosphorus speciation in mature wheatand canola plants as afected by phosphorus supply," Plant andSoil, vol. 378, no. 1-2, pp. 125–137, 2014.

[28] F. S. Higashikawa, C. A. Silva, and W. Bettiol, "Chemical andphysical properties of organic residues," Revista Brasileira deCiencia do Solo ˆ, vol. 34, no. 5, pp. 1743–1752, 2010.

[29] C. Nzila, D. Njuguna, D. Madara et al., "Characterization ofagro-residues for biogas production and nutrient recovery inKenya," Journal of Emerging Trends in Engineering and AppliedSciences (JETEAS), vol. 6, no. 5, pp. 327–334, 2015.

[30] K. Naklang, A. Whitbread, R. Lefroy et al., "Te managementof rice straw, fertilisers and leaf litters in rice cropping systemsin Northeast Tailand: I. Soil carbon dynamics," Plant and Soil,vol. 209, no. 1, pp. 21–28, 1999.

[31] B. L. Turner, M. J. Paphazy, P. M. Haygarth, and I. D. McKelvie, ´"Inositol phosphates in the environment," Philosophical Trans actions of the Royal Society B: Biological Sciences, vol. 357, no.1420, pp. 449–469, 2002.

[32] M. I. Makarov, L. Haumaier, W. Zech, O. E. Marfenina, and L.V. Lysak, "Can 31P NMR spectroscopy be used to indicate theorigins of soil organic phosphates?" Soil Biology & Biochemistry,vol. 37, no. 1, pp. 15–25, 2005.

[33] D. T. Mitchell and N. Allsopp, "Changes in the phosphoruscomposition of seeds of hakea sericea (proteaceae) during germination under low phosphorus conditions," New Phytologist,vol. 96, no. 2, pp. 239–247, 1984.

[34] N. R. Reddy, M. D. Pierson, S. K. Sathe, and D. K. Salunkhe,Phytates in Cereals and Legumes, CRC Press, Inc, Boca Raton,Florida, 1989.

[35] K. B. Adejobi, A. O. Famaye, O. S. O. Akanbi, S. A. Adeosun,A. B. Nduka, and D. O. Adeniyi, "Potentials of cocoa pod huskash as fertilizer and liming materials on nutrient uptake andgrowth performance of cocoa," Research Journal of Agricultureand Environmental Management, vol. 2, no. 9, pp. 243–251, 2013.

[36] A. Kornberg, "Inorganic polyphosphate: a molecule of manyfunctions.," Progress in Molecular and Subcellular Biology, vol.23, pp. 1–18, 1999.

[37] A. L. Doolette, R. J. Smernik, and W. J. Dougherty, "Spikingimproved solution phosphor us-31 nuclear magnetic resonanceidentifcation of soil phosphorus compounds," Soil ScienceSociety of America Journal, vol. 73, no. 3, pp. 919–927, 2009.

[38] B. L. Turner, B. J. Cade-Menun, and D. T.Westermann, "Organicphosphorus composition and potential bioavailability in semi arid arable soils of the Western United States," Soil ScienceSociety of America Journal, vol. 67, no. 4, pp. 1168–1179, 2003

A Simple Incorporation Route of Tris(8-hydroxyquinoline)aluminum(III) into Transparent Mesoporous Silica Films and Their Photofunctions

Motohiro Tagaya,1 Kenji Shinozaki,2 and Yuri Maruko1

1 Department of Materials Science and Technology, Nagaoka University of Technology, 1603-1 Kamitomioka,
Nagaoka, Niigata 940–2188, Japan

2 National Institute of Advanced Industrial Science and Technology (AIST), 1-8-31 Midorigaoka, Ikeda, Osaka 563–8577, Japan

INTRODUCTION

Studies on the incorporation of functional organic molecules into porous inorganic solids have been extensively conductedto construct the functional inorganic-organic supramolec ular nanosystems [1]. The molecular aggregation/dispersionstates of functional guest species on the well-definedmesostructures affect the physicochemical properties of thehost-guest hybrids. The controlled adsorption properties onthe various inorganic supports [2–7] are known to give themerits of the immobilization of functional units. Accordingly,the host-guest and guest-guest interactions are importantfactors to offer the multiple possibilities, so that the systematicstudies on the design and characterization of the hybrids byvarious compositions and different nanostructures are worth conducting.

After the discovery of mesoporous silica (MPS) prepared by the cooperative organization of surfactant and inorganicspecies, the synthesis, characterization, and applications ofthe mesostructured materials have extensively been inves tigated. The MPS prepared by supramolecular templatingmethods [8, 9] possesses attractive features such as well defined and controllable pore sizes, large surface areas, andreactive surfaces for the guest organization. The effect of theguest confinement into the nanospaces on the photophysicalproperties has been investigated [10]. In addition to thehost-guest interactions, the guest-guest interactions can becontrolled. Accordingly, the host-guest complexes based onMPS have been synthesized, and the possible applicationsfor optical materials have been reported [11–13]. Although awide variety of host-guest complexes have been synthesized,the possible effect of pore size on the photo functions ha shardly been reported. Furthermore, the processing of the photofunctional mesostructures with controlled morphologyis a basic prerequisite for the applications. Accordingly, thecontrolled macroscopic morphologies, such as films [14–18],

particles [19–21], and monoliths [22, 23] with the mesostructures, have been suggested as the host-guest complexes.

In this study, we investigated the adsorption of tris(8-hydroxyquinoline)aluminum(III) (Alq), which has been studied as an organic light-emitting material [24], into the MPS films with different pore sizes (3.0 and 5.4 nm) prepared from cationic and nonionic surfactants to clarify the molecular aggregation/dispersion states of Alq at the film mesopore structures. It is known that the photoluminescence characteristics of bulk state depend on the Alq crystalline phases (α, β, γ, etc.) and molecular packing [25–28], and these parameters have been controlled by synthetic pathways as well as by postsynthetic treatments, indicating that the crystalline phase is associated with the luminescence properties of Alq. Although the effects of the morphologies of neat Alq on the performance of the devices have been intensively investigated [29–31], the effective control of the intermolecular interactions of Alq has not been well-documented. Therefore, the control of the intermolecular interactions of Alq as well as the interactions between Alq and mesopore surfaces is the possible way to understand the correlation between the intermolecular interactions of Alq and the luminescence. We have already found that the Alq was easily occluded into the MPS powders from solutions [32, 33], suggesting the importance of the host-guest interactions between MPS and Alq. In the present study, we conducted the adsorption of Alq into the transparent MPS films with the different pore sizes and investigated the states of the Alq.

2. Experimental

2.1. Preparation of Mesoporous Silica Films and Their Alq Complexation. In order to compare the interactions between the adjacent Alq molecules with the interactions between Alq and mesopores, the MPS with Barrett-Joyner-Halenda (BJH) [34] pore sizes of 3.0 and 5.4 nm was prepared using the different template surfactants of octadecyltrimethylammonium chloride (C_{18}TAC, Tokyo Chemical Industry (TCI) Co., Ltd.) and triblock poly(ethylene oxide (EO))-poly(propylene oxide (PO))-poly(ethylene oxide (EO)) copolymer ($EO_{20}PO_{70}EO_{20}$, Aldrich Co., Ltd.) denoted by P123. Here, the MPS with the pore sizes of 3.0 and 5.4 nm was designated as C18MPS-3.0 and P123MPS-5.4, respectively.

C18MPS-3.0 film was synthesized based on the previous report [14, 18]. 1.94 mL of tetramethoxysilane (TMOS, TCI Co., Ltd.), ultrapure water (472 μL), and hydrochloric acid aqueous solution (0.1 N, 100 μL) were mixed at 313 K for 1 h. Then, 534 mg of C_{18}TAC was dispersed into ultrapure water (1.4 mL) at 313 K, and the siliceous solution was added to the surfactant solution and immediately 100 μL of hydrochloric acid aqueous solution (1 N) was added to the mixed solution and stirred at 313 K. In contrast, P123MPS-5.4 film was synthesized based on the modified previous report [35]. 1.12 mL of tetraethoxysilane (TEOS, TCI Co., Ltd.), ultrapure water (130 μL), ethanol (1121 μL), and hydrochloric acid aqueous solution (1 N, 29 μL) were mixed and stirred at 333 K. Then, 252 mg of P123 was dispersed into hydrochloric acid aqueous solution (0.01 N, 415 μL), and the siliceous solution was added to the surfactant solution and stirred at room temperature for 2 h.

These resulting solutions were spin-coated on a glass substrate at a rotation speed of 6000 rpm and then dried at 333 K for 18 h. The supramolecular templates were removed by the calcination at 723 K for 6 h, which was confirmed by a Fourier transform infrared (FT-IR) spectroscopy.

2.2. Preparation of Alq Powders. The solvated Alq powders were prepared using a vacuum concentration method from the ethanol or benzene solution, suggesting the recrystallization of the ethanol-Alq and benzene-Alq powders [26]. By the morphological observation of the powders by an optical microscopy, it was confirmed that the crystal shapes and sizes from benzene were more homogeneous and smaller. Accordingly, the benzene solution was used in this study. The Alq crystals recrystallized on the C18MPS-3.0 and P123MPS-5.0 film and glass substrate surfaces were prepared from the higher Alq concentration in benzene at 1.2 mM.

2.3. Adsorption of Alq into MPS Films. The adsorption of Alq (α-phase powder, TCI Co., Ltd.) into the MPS films was conducted by the admixture of the MPS films (dried at 393 K for 4 h under dry air) with benzene solution of Alq with the different concentrations at room temperature for 1 h. The resulting films were physically washed by ultrapure water and dried under reduced pressure for 1 day and were designated as Alq/C18MPS-3.0 and Alq/P123MPS-5.4.

2.4. Characterization. The surface nanostructures were analyzed by an atomic force microscope (AFM: Nanocute, SII Investments, Inc.) in areas of 0.5 × 0.5 and 5.0 × 5.0 μm^2. The surface roughness (R_{rms}) was calculated by the root mean squares in the height images. X-ray diffraction (XRD) patterns were recorded with a powder X-ray diffractometer (Smart Lab, Rigaku, Japan) equipped with monochromatic CuKα radiation operated at 20 mA and 40 kV. The nitrogen adsorption isotherms of the films were measured at 77 K on an BELSORP-miniII instrument (MicrotracBEL Co., Ltd.) to calculate Brunauer–Emmett–Teller (BET) surface areas [36] and BJH pore size distributions. Prior to the measurement, a number of samples were degassed under vacuum at 393 K for 4 h.

The adsorbed amount of Alq in the MPS was determined by the change in the concentration of Alq in the solution before and after the reaction, which was determined by the changes of absorbance of Alq in benzene at 377 nm using a UV-visible absorption spectroscopy (V-750, JASCO Co., Ltd.). The adsorption amount at the equilibrium state (W) was calculated by (1) based on the adsorption isotherms. On the basis of the Langmuir adsorption isotherm formula, the equation of state for the one-component adsorption can be represented as follows:

$$\frac{C}{W} = \frac{1}{(K_{eq} \cdot W_{max})} + \left(\frac{1}{W_{max}}\right) C, \quad (1)$$

where C, K_{eq}, and W_{max} are the Alq concentration in the equilibrium state, the adsorption equilibrium constant, and

the maximum adsorption amount, respectively. K_{eq} and W_{max} were determined from the slope of a C/W versus C plot. The Alq adsorption based on the correlation coefficient was found to be Langmuir type monolayer adsorption.

The photoluminescence spectra were recorded on a FP-8500 spectrophotometer (JASCO Co., Ltd.) with the excitation wavelength at 365 nm (atmosphere: air, excitation-slit/detection-slit: 2 nm/2 nm, measure time: 0.1 s, step width: 1.0 nm, sample weight: 150 mg, and shape: pellet), and the detection was used by photomultiplier tube. A cryostat was used to obtain the temperature-dependent photoluminescence spectra between 80 and 300 K. The inside temperature was controlled using a heater in conjunction with the cryostat. All the photoluminescence spectra were measured through a quartz window. From the spectra, the integrated luminescence intensity (I) was calculated by the areas in the range between 420 and 670 nm, and I per 1 mol of Alq was calculated by dividing I by the adsorbed molar amount of Alq on the MPS films. The intensity maxima among the MPS with the different adsorbed amount of Alq were fixed to be 1.0. The integrated luminescence intensities centered at the peak tops of 462 and 525 nm, which are abbreviated as I_{462} and I_{525}, were calculated based on the Gaussian-function deconvolution and fitting to obtain the I_{525}/I_{462} values. In the deconvolution, the components and peak positions were initially fixed and then were refined only for the peak heights. During the final optimization, only the components and peak widths were refined again to reduce the residual values. The luminescence microscope image of the MPS adsorbed Alq was obtained by a CKX41N-FL photoluminescence microscope (OLYMPUS Co., Ltd., excitation wavelength: 360–400 nm, exposure time: 100 ms) through the emission source (OLYMPUS Co., Ltd., U-RFLT50).

3. Results and Discussion

Figure 1 shows the AFM images of the MPS film surfaces and their nitrogen adsorption and desorption isotherms and BJH pore size distributions. The surface structures are particulate and the domain size of P123MPS-5.4 was larger than that of C18MPS-3.0, which were also seen in the phase-shift images (see Figure S1 in Supplementary Material available online at https://doi.org/10.1155/2017/7351263), and R_{rms} of the C18MPS-3.0 and P123MPS-5.4 films were 1.6 and 2.6 nm, respectively. In the nitrogen adsorption and desorption isotherms, the hysteresis loops between the adsorption and desorption processes were observed. According to the IUPAC classification [37], the isotherm and hysteresis classifications were indexed as type IV and H4 for C18MPS-3.0 and type IV and H1 for P123MPS-5.4, indicating the existence of mesopores. The BET surface area of C18MPS-3.0 was higher than that of P123MPS-5.4 as shown in Table 1. The BJH pore size distributions indicate the mesopore range up to approximately 15 nm. Therefore, the different surface structures were successfully prepared. It was suggested that the BJH pore sizes of 3.0 and 5.4 nm are large enough to accommodate Alq when the hydrodynamic space by molecular diffusion in addition of the distance between Alq and silanol group in the mesopore is considered.

Figure 2 shows the fluorescent microscope images and photoluminescence spectra of the solvated Alq powders before and after the recrystallization. The morphologies of α-Alq, ethanol-Alq, and benzene-Alq crystals were needle, cuboid, and plate-like shapes, respectively, and the crystal shape and size from benzene were more homogeneous and smaller. Moreover, the luminescence maximum of benzene-Alq was longer region as compared with those of the other crystals, indicating the strong Alq-benzene packing interactions. These results would be attributed to the solvent polarity. In the case of benzene, the π-π interactions were thought to be enhanced through the intervention of the solvent molecules [26]. Thus, benzene was used as the adsorption solvent in the following experiments.

Figure 3(a) shows the adsorption isotherms of Alq into the MPS films. The adsorbed amounts were controlled by changing the added amount of Alq in solution. The adsorption isotherm of the Alq into C18MPS-3.0 could be classified as a Langmuir type [38], indicating the strong adsorbent-adsorbate interaction. When P123MPS-5.4 was used, the adsorption isotherm was S type, indicating the weaker adsorbent-adsorbate interaction. As shown in Table 1, the adsorption properties were different between the MPS host and the W_{max}/S_{BET}, which denotes the amount of adsorbed Alq per the experimentally determined BET surface area. W_{max}/S_{BET} observed for P123MPS-5.4 was smaller as compared with that for C18MPS-3.0, suggesting that the host-guest interactions are clearly different depending on the pore size and templating surfactant. Generally, the uncondensed hydroxyl groups on the silica surface induce polar nature on the surface. Thus, Alq was electrostatically captured on the silica surface by hydrogen-bonding interactions with silanol groups. After drying, the Alq molecules adhered to the pore

argue that the "host-guest interactions" were successfully formed at the mesopores.

In the adsorption process at the higher Alq solution (1.2 mM), the segregation of the Alq crystals grown on the C18MPS-3.0 and P123MPS-5.4 films was observed (Figures 3(b) and 3(c)), suggesting that the adsorption behavior dominantly occurs at the concentration less than 1.2 mM. The morphologies of crystals depend on the MPS, and that on P123MPS-5.4 (Figure 3(c)) was clearly different from those on the C18MPS-3.0 (Figure 3(b)) and glass (Supplementary Material, Figure S2). These results indicate that the molecular stacking structures were dominantly originated from the inside and/or outside mesopore surface properties.

Figures 4(a) and 4(b) show the XRD patterns of C18MPS-3.0, Alq/C18MPS-3.0, P123MPS-5.4, and Alq/P123MPS-5.4 films. The X-ray diffraction patterns suggested that the ordered hexagonal mesopore arrangements are preserved with the adsorption of Alq. Alq was adsorbed effectively into the films to apparently give transparently yellow-color, and the photographs of the films with the maximum adsorbed amounts of Alq in Figures 4(c) and 4(d) indicate the preservation of transparency with the adsorption. The AFM topographic images in Figures 4(e) and 4(f) clearly exhibited no segregation on the films, which were also seen in the phase-shift images (Supplementary Material, Figure S3), and

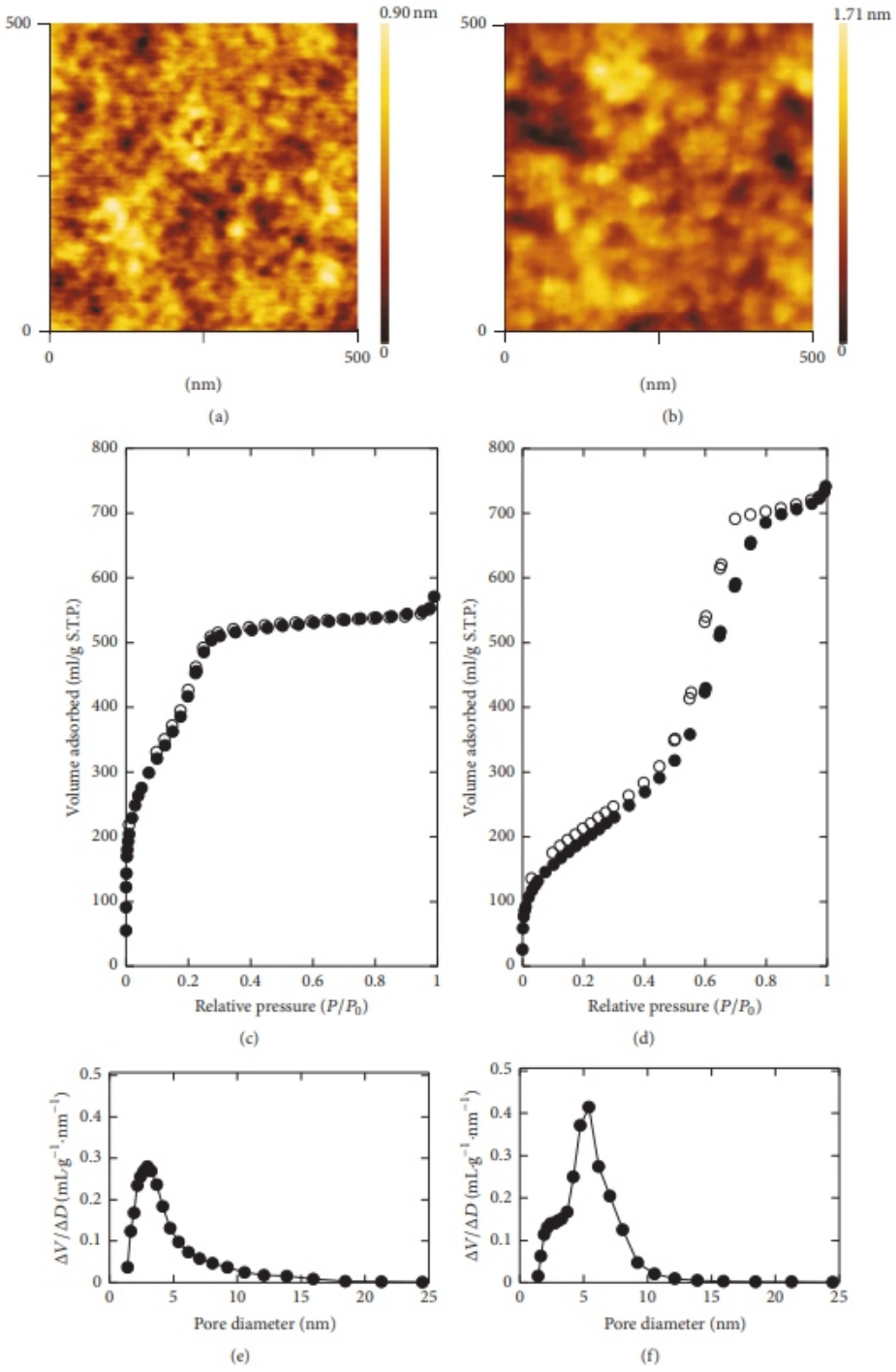

Figure 1: (a, b) AFM topographic images (observation area: 500 nm2), (c, d) nitrogen adsorption (open symbols) and desorption (closedsymbols) isotherms, and (e, f) BJH pore size distributions of (a, c, e) C18MPS-3.0 and (b, d, f) P123MPS-5.4 films

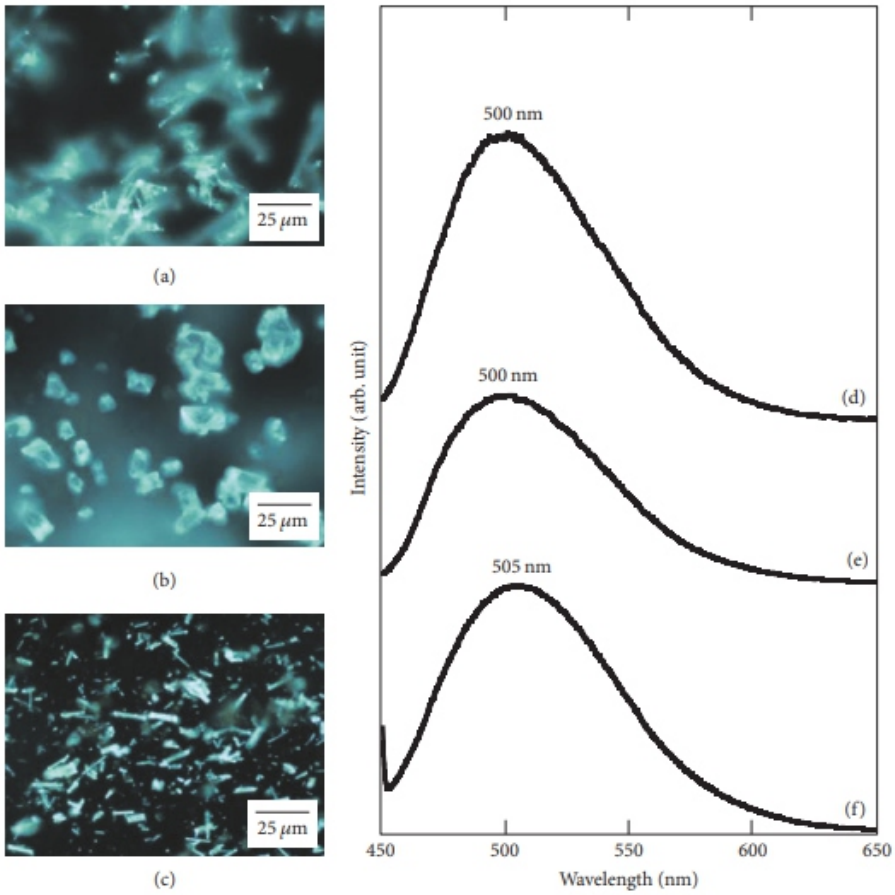

FIGURE 2: (a–c) Fluorescent microscope images and (d–f) photoluminescence spectra of (a, d) neat Alq powder and solvated Alq powders recrystallized from (b, e) ethanol and (c, f) benzene.

TABLE 1: S_{BET} and r_{BJH} of the C18MPS-3.0 and P123MPS-5.4 films and the adsorption properties of Alq (W_{max}, W_{max}/S_{BET}, K_{eq}) from the adsorption isotherms by the saturation method based on Langmuir equation.

	Mesopore properties		Adsorption properties of Alq into MPS		
	S_{BET} ($m^2\ g^{-1}$)	r_{BJH} (nm)	W_{max} (μmol·(g of MPS)$^{-1}$)	W_{max}/S_{BET} (Molecules·(nm^2 of MPS)$^{-1}$)	K_{eq} ($10^{-3}\ M^{-1}$)
C18MPS-3.0	1089	3.0	300	0.16	18.1
P123MPS-5.4	742	5.4	150	0.12	6.7

R_{rms} values of the Alq/C18MPS-3.0 and Alq/P123MPS-5.4 films were 5.2 and 4.6 nm, respectively.

In order to discuss the state of the Alq molecules in the mesopore, the photoluminescence spectra of the Alq adsorbed in the MPS films were investigated as a function of the adsorbed amount of Alq. Figures 5(a) and 5(b) show the luminescence spectra of the Alq/C18MPS-3.0 and Alq/P123MPS-5.4 films with the different adsorbed amount. When the adsorbed amount of Alq was smaller, the luminescence bands split into 462 and 525 nm. At the maximum adsorbed amounts, the luminescence maxima were observed at 510 nm for C18MPS-3.0 and 513 nm for P123MPS-5.4 without the spectral split. I increased with increasing the adsorbed amount of Alq (Figure 5(c)). The changes in I per 1 mol of Alq exhibited the minimal luminescence intensity regions (Figure 5(d)). Considering the increase in the intensity at around 525 nm region (Figure 5(e)), it was thought that the guest-guest interactions (e.g., long-period π-π interactions [26]) were changed to be dominated above the threshold amount of adsorbed Alq. I per 1 mol of Alq in the P123MPS-5.4 film was higher at the maximum adsorption amount of Alq. When P123MPS-5.4 was used as the host, the luminescence was observed at the longer wavelength, suggesting that the larger pore size enabled the adsorbed Alq to aggregate even at the low Alq concentration. As shown in inset fluorescent microscope images, the Alq/C18-MPS and

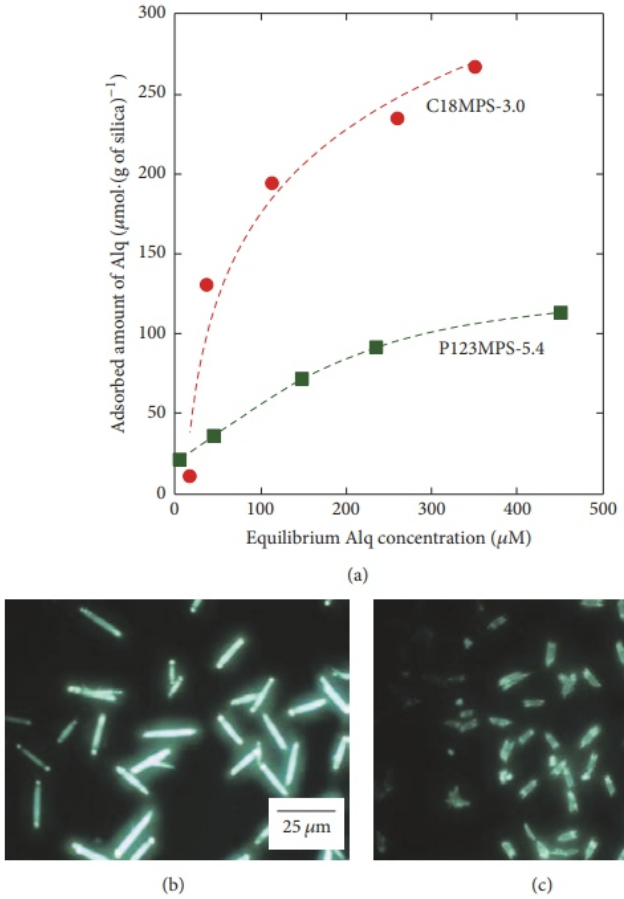

FIGURE 3: (a) Adsorption isotherms of Alq into C18MPS-3.0 and P123MPS-5.4 from benzene solution. Fluorescent microscope images of the segregation Alq crystals grown on (b) C18-MPS and (c) P123-MPS films, which were precipitated under the higher Alq concentration in benzene at 1.2 mM.

Alq/P123-MPS films with the maximum adsorption amount of Alq homogeneously exhibited the green luminescence. This is the first time to successfully prepare the Alq-silica complex films.

Considering the luminescence maxima of Alq in benzene at 517 nm, ethanol at 515 nm, and methanol at 514 nm [26] and their monomodal spectral shapes, it is suggested that the state of Alq molecules in the mesopores was different from that in the solution state. From the spectral variation of the crystalline Alq, the luminescence red-shift was ascribed to the shorter interligand distance and/or the denser molecular packing of Alq [26]. Based on the other reports [27, 28], the luminescence at around 470 and 520 nm was ascribed to the delta or gamma crystalline phase of Alq arranged in a manner minimizing the overlap of the π-orbitals between pairs of hydroxyquinoline ligands belonging to neighboring Alq molecules and to the amorphous state which formed the favorable overlap of facing the ligands, respectively [32]. Accordingly, we have ascribed the two bands at 462 and 525 nm to isolated and aggregated Alq in the mesopore, respectively [21]. The bimodal peak variations of the relative luminescence intensity (I_{525}/I_{462}) as a function of the adsorbed amount of Alq are shown in Figure 5(e). I_{525}/I_{462} varied depending on the adsorbed amounts of Alq and increased gradually for C18MPS-3.0 and dramatically for P123MPS-5.4, suggesting that the intermolecular interactions among Alq molecules were enhanced by the P123MPS-5.4 host. It is thought that the strong interactions between Alq and mesopore surface led to the adsorption of Alq as isolated molecular states at the lower adsorbed amounts and then the intermolecular interactions enhanced upon crowding as suggested in Figure 6. It was supposed that nonionic P123-templated mesopore surfaces with the smaller amount of silanol groups affected the crowding of Alq (i.e., guest-guest interactions) at the lower concentrations. Therefore, the state of Alq in the mesopore with the amount of adsorbed Alq apparently varied depending on the pore size as well as the surface properties based on templating surfactants.

The photoluminescence spectral changes, the integrated intensity, and maxima plots with the temperature range

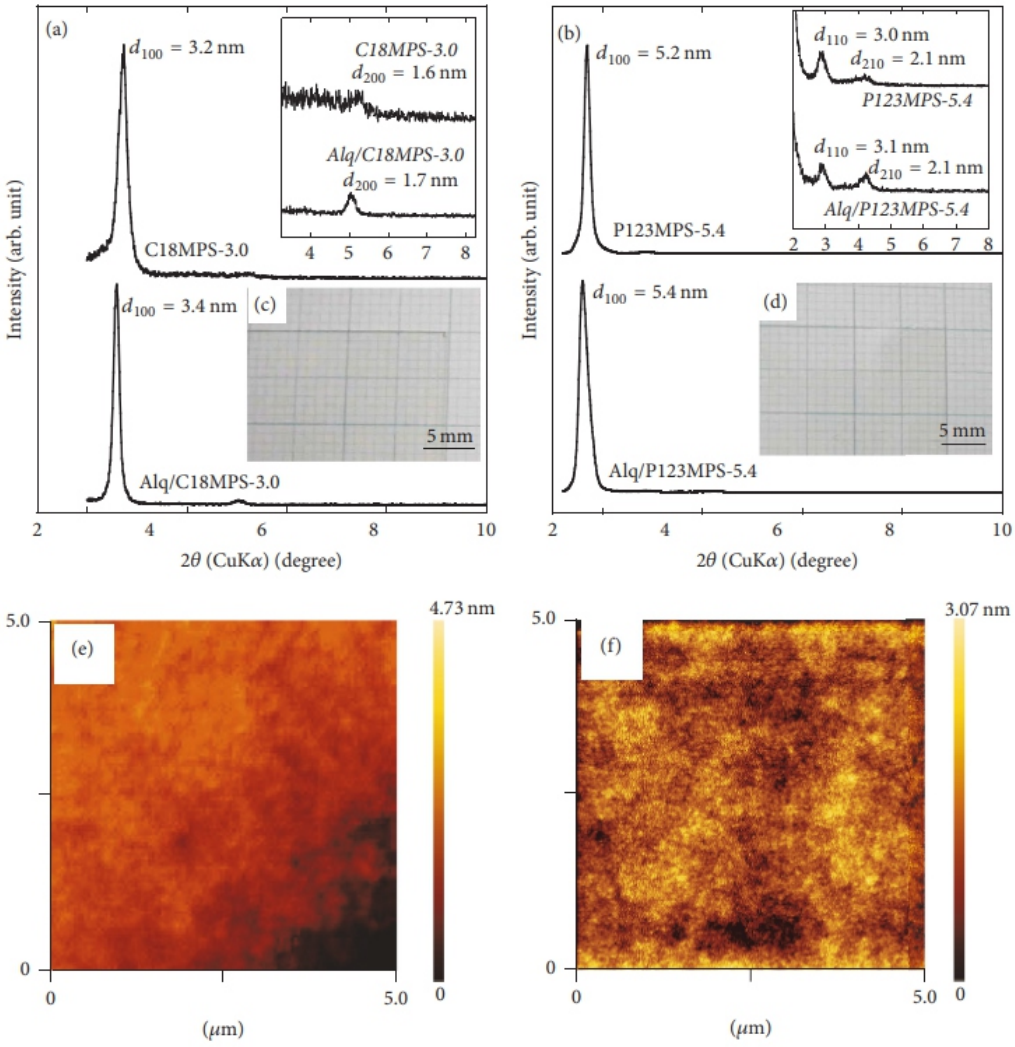

FIGURE 4: XRD patterns of (a) C18MPS-3.0 and Alq/C18MPS-3.0 and (b) P123MPS-5.4 and Alq/P123MPS-5.4 films (insets: the magnified patterns at 2θ = 3.25–8.25° regions). The Alq/C18MPS-3.0 and Alq/P123MPS-5.4 films with the adsorbed amounts of Alq at 267 and 117 μmol/(g of MPS) were evaluated by (c, d) photographs and (e, f) AFM topographic images (observation area: 5.0 μm^2).

between 80 and 300 K of α-Alq powder, Alq/C18MPS-3.0, and Alq/P123MPS with the adsorbed amount of Alq at 131 and 91 μmol/g, respectively, were shown in Figure S4 (Supplementary Material). In Figure S4(d–f), the y-axis was the relative luminescence intensity normalized to that at 300 K. For α-Alq powder (Figure S4(a, d)), the increase in the luminescence intensity as the temperature decreases from 300 to 80 K was observed, and these changes were reversible. Similar changes have also been reported previously for the neat Alq powders and films, which were attributed to only the reduction of the temperature quenching [39, 40]. No vibronic structures in the spectra appeared below 150 K, suggesting that the ordering structures of the Alq molecules were preserved by the temperature changes. For the Alq adsorbed in the MPS films, the integrated luminescence intensity increased and the spectral red and blue shifts by C18MPS-3.0 and P123MPS-5.4 were observed with decreasing temperature from 300 to 80 K, and these changes were reversible. The intensity increased with the temperature variation (the maximum intensity at 80 K) which was observed without exhibiting vibronic structure in the spectra. The luminescence changes of the Alq adsorbed in the MPS films were different from α-Alq and depended on the host. It has been reported that the δ- and γ-crystalline phases showed the blue-shifted luminescence maximum at near 470 nm and have the well-defined molecular arrangements in comparison with those of other phases (α- and β-phases, amorphous state) [27, 28]. The rearrangement of Alq molecules in the mesopore altered from the disorder with the enhanced intermolecular interactions to the δ- and γ-crystal-like states using the P123MPS-5.4 host, and the reverse alternation occurred using the C18MPS-3.0 host. Judging from the results, the states of the adsorbed Alq in the MPS films altered in the temperature variations, which depended on the pore size as

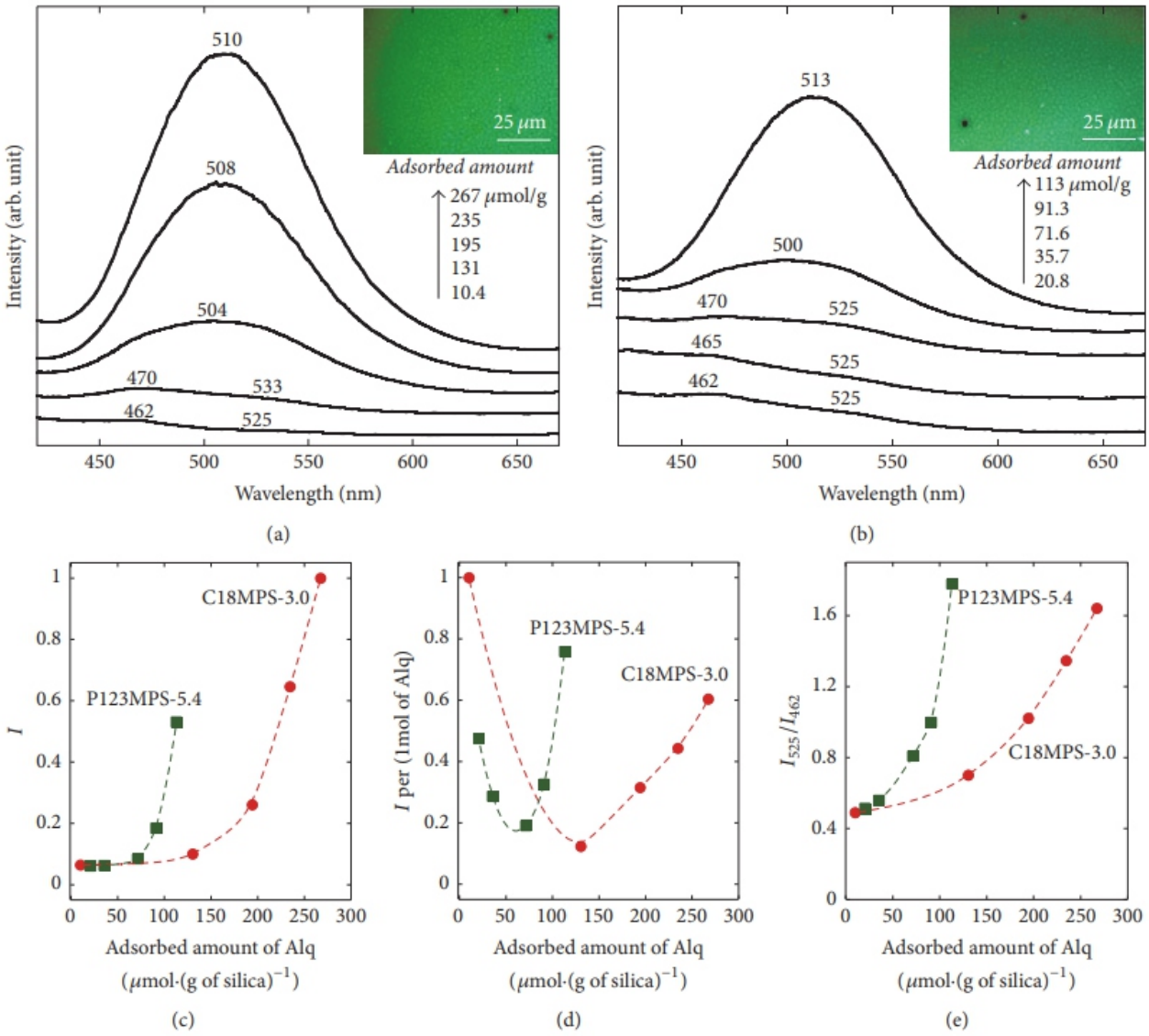

FIGURE 5: Photoluminescence spectra of (a) Alq/C18MPS-3.0, (b) Alq/P123MPS-5.4 films with the different adsorbed amounts of Alq (insets: fluorescent microscope images of the Alq/C18MPS-3.0 and Alq/P123MPS-5.4 films with the adsorbed amount of Alq at 267 and 117 μmol/(g of MPS), resp.), (c) I, (d) I per 1 mol, and (e) I_{525}/I_{462} changes with the adsorbed amount.

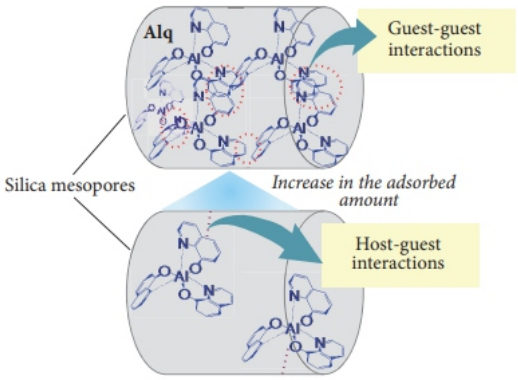

FIGURE 6: Possible host-guest and guest-guest interaction changes with increasing the adsorbed amount of Alq in the mesospores.

well as the adsorbed amount of Alq. In particular, P123MPS-5.4 exhibited the characteristic luminescence behavior with the temperature variation if compared with the case in the C18MPS-3.0. Therefore, the effective nanospace confinement of Alq was clarified by controlling the molecular states in the mesopores.

4. Conclusion

Alq was successfully adsorbed without segregation into the MPS films with the different pore sizes. The adsorbed amount was controlled by changing the added amount in the initial solution to resultantly exhibit the transparent and yellow-color films. The molecular states of Alq in the mesopore varied upon the adsorbed amount of Alq as well as the surface properties of the mesospores. The luminescence of the adsorbed Alq revealed that the rearrangements of the molecules in the mesopore occurred to exhibit the significant aggregation/disaggregation between the molecules. Therefore, the MPS surfaces effectively controlled the guest-guest interactions between the Alq molecules as well as the host-guest interactions between the Alq and mesopore. This finding by the use of the mesoporous hosts will be utilized for including luminescence species and be applicable for optical devices.

Conflicts of Interest

There are no conflicts of interest regarding the publication of this paper.

Acknowledgments

This study was supported by a grant from the Japan Society for the Promotion of Science (JSPS) KAKENHI (Grant-in-Aid for Young Scientists (A), Grant no. 17H04954, and Challenging Research (Exploratory), Grant no. 17K19027). The authors thank Analysis and Instrumentation Center in Nagaoka University of Technology for providing the facilities. The authors thank Professor Dr. Makoto Ogawa for many helpful discussions.

References

[1] M. Ogawa, "6 Organized molecular assemblies on the surfaces of inorganic solids - photofunctional inorganic-organic supramolecular systems," *Annual Reports on the Progress of Chemistry - Section C*, vol. 94, pp. 209–257, 1998.

[2] M. J. Wirth, R. W. P. Fairbank, and H. O. Fatunmbi, "Mixed self-assembled monolayers in chemical separations," *Science*, vol. 275, no. 5296, pp. 44–47, 1997.

[3] M. Ogawa, "Control of interlayer microstructures of a layered silicate by surface modification with organochlorosilanes [8]," *Journal of the American Chemical Society*, vol. 120, no. 29, pp. 7361-7362, 1998.

[4] A. Slama-Schwok, M. Ottolenghi, and D. Avnir, "Long-lived photoinduced charge separation in a redox system trapped in a sol-gel glass," *Nature*, vol. 355, no. 6357, pp. 240–242, 1992.

[5] M. Tagaya, T. Ikoma, Z. Xu, and J. Tanaka, "Synthesis of luminescent nanoporous silica spheres functionalized with folic acid for targeting to cancer cells," *Inorganic Chemistry*, vol. 53, no. 13, pp. 6817–6827, 2014.

[6] J. Kerry Thomas, "Physical aspects of photochemistry and radiation chemistry of molecules adsorbed on SiO2, γ-Al2O3, zeolites, and clays," *Chemical Reviews*, vol. 93, no. 1, pp. 301–320, 1993.

[7] K. B. Yoon, "Electron- and charge-transfer reactions within zeolites," *Chemical Reviews*, vol. 93, no. 1, pp. 321–339, 1993.

[8] T. Yanagisawa, T. Shimizu, K. Kuroda, and C. Kato, "The preparation of alkyltrimethylammonium-kanemite complexes and their conversion to microporous materials," *Bulletin of the Chemical Society of Japan*, vol. 63, no. 4, pp. 988–992, 1990.

[9] C. T. Kresge, M. E. Leonowicz, W. J. Roth, J. C. Vartuli, and J. S. Beck, "Ordered mesoporous molecular sieves synthesized by a liquid-crystal template mechanism," *Nature*, vol. 359, no. 6397, pp. 710–712, 1992.

[10] M. Ogawa, "Photoprocesses in mesoporous silicas prepared by a supramolecular templating approach," *Journal of Photochemistry and Photobiology C: Photochemistry Reviews*, vol. 3, no. 2, pp. 129–146, 2002.

[11] K. Moller and T. Bein, "Inclusion chemistry in periodic mesoporous hosts," *Chemistry of Materials*, vol. 10, no. 10, pp. 2950–2963, 1998.

[12] A. Stein, B. J. Melde, and R. C. Schroden, "Hybrid inorganic-organic mesoporous silicates-nanoscopic reactors coming of age," *Advanced Materials*, vol. 12, no. 19, pp. 1403–1419, 2000.

[13] B. J. Scott, G. Wirnsberger, and G. D. Stucky, "Mesoporous and mesostructured materials for optical applications," *Chemistry of Materials*, vol. 13, no. 10, pp. 3140–3150, 2001.

[14] M. Ogawa, "Formation of novel oriented transparent films of layered silica-surfactant nanocomposites," *Journal of the*

[15] M. Ogawa, "A simple sol-gel route for the preparation of silica-surfactant mesostructured materials," *Chemical Communications*, no. 10, pp. 1149-1150, 1996.

[16] K. M. McGrath, D. M. Dabbs, N. Yao, I. A. Aksay, and S. M. Gruner, "Formation of a silicate L3 phase with continuously adjustable pore sizes," *Science*, vol. 277, no. 5325, pp. 552–556, 1997.

[17] Y. Lu, R. Ganguli, C. A. Drewien et al., "Continuous formation of supported cubic and hexagonal mesoporous films by sol-gel dip-coating," *Nature*, vol. 389, no. 6649, pp. 364–368, 1997.

[18] M. Tagaya, K. Kobayashi, and M. Nishikawa, "Additive effect of phosphoric acid on phosphorus-containing mesoporous silica film formation," *Materials Letters*, vol. 164, pp. 651–654, 2016.

[19] H.-P. Lin and C.-Y. Mou, "Tubules-within-a-tubule hierarchical order of mesoporous molecular sieves in MCM-41," *Science*, vol. 273, no. 5276, pp. 765–768, 1996.

[20] Q. Huo, J. Feng, F. Schüth, and G. D. Stucky, "Preparation of hard mesoporous silica spheres," *Chemistry of Materials*, vol. 9, no. 1, pp. 14–17, 1997.

[21] M. Tagaya, S. Motozuka, T. Kobayashi, T. Ikoma, and J. Tanaka, "Efficient incorporation of monomeric anthracene into nanoporous silica/surfactant nanocomposite spheres using a mechanochemical solid state reaction," *Journal of Materials Chemistry*, vol. 22, no. 36, pp. 18741–18743, 2012.

[22] N. A. Melosh, P. Lipic, F. S. Bates et al., "Molecular and mesoscopic structures of transparent block copolymer-silica monoliths," *Macromolecules*, vol. 32, no. 13, pp. 4332–4342, 1999.

[23] M. Tagaya, N. Hanagata, and T. Kobayashi, "Templating effect of mesostructured surfactant-silica monolithic films on the

surface structural and mechanical properties," *ACS Applied Materials and Interfaces*, vol. 4, no. 11, pp. 6169–6175, 2012.

[24] C. W. Tang and S. S. van Slyke, "Organic electroluminescent diodes," *Applied Physics Letters*, vol. 51, no. 12, pp. 913–915, 1987.

[25] J.-J. Chiu, C.-C. Kei, T.-P. Perng, and W.-S. Wang, "Organic semiconductor nanowires for field emission," *Advanced Materials*, vol. 15, no. 16, pp. 1361–1364, 2003.

[26] M. Brinkmann, G. Gadret, M. Muccini, C. Taliani, N. Masciocchi, and A. Sironi, "Correlation between molecular packing and optical properties in different crystalline polymorphs and amorphous thin films of *mer*-tris(8-hydroxyquinoline)aluminum(III)," *Journal of the American Chemical Society*, vol. 122, no. 1, pp. 5147–5157, 2000.

[27] M. Cölle, J. Gmeiner, W. Milius, H. Hillebrecht, and W. Brütting, "Preparation and characterization of blue-luminescent tris(8-hydroxyquinoline)aluminum (Alq_3)," *Advanced Functional Materials*, vol. 13, no. 2, pp. 108–112, 2003.

[28] H. Kaji, Y. Kusaka, G. Onoyama, and F. Horii, "CP/MAS ^{13}C NMR characterization of the isomeric states and intermolecular packing in tris(8-hydroxyquinoline) aluminum(III) (Alq_3)," *Journal of the American Chemical Society*, vol. 128, no. 13, pp. 4292–4297, 2006.

[29] C. P. Cho, C. A. Wu, and T. P. Peng, "Crystallization of amorphous tris(8-hydroxyquinoline)aluminum nanoparticles and transformation to nanowires," *Advanced Functional Materials*, vol. 16, pp. 819–823, 2006.

[30] G. M. Credo, D. L. Winn, and S. K. Buratto, "Near-field scanning optical microscopy of temperature- and thickness-dependent morphology and fluorescence in Alq3 films," *Chemistry of Materials*, vol. 13, no. 4, pp. 1258–1265, 2001.

[31] D. S. Qin, D. C. Li, Y. Wang et al., "Effects of the morphologies and structures of light-emitting layers on the performance of organic electroluminescent devices," *Applied Physics Letters*, vol. 78, no. 4, pp. 437–439, 2001.

[32] M. Tagaya and M. Ogawa, "Luminescence of tris(8-quinolinato)aluminum(III) (Alq3) adsorbed into mesoporous silica," *Chemistry Letters*, vol. 35, no. 1, pp. 108-109, 2006.

[33] M. Tagaya and M. Ogawa, "Possible pore size effects on the state of tris(8-quinolinato)aluminum(iii) (Alq3) adsorbed in mesoporous silicas and their temperature dependence," *Physical Chemistry Chemical Physics*, vol. 10, no. 45, pp. 6849–6855, 2008.

[34] E. P. Barrett, L. G. Joyner, and P. P. Halenda, "The determination of pore volume and area distributions in porous substances. I. Computations from nitrogen isotherms," *Journal of the American Chemical Society*, vol. 73, no. 1, pp. 373–380, 1951.

[35] D. Zhao, P. Yang, N. Melosh, J. Feng, B. F. Chmelka, and G. D. Stucky, "Continuous mesoporous silica films with highly ordered large pore structures," *Advanced Materials*, vol. 10, no. 16, pp. 1380–1385, 1998.

[36] S. Brunauer, P. H. Emmett, and E. Teller, "Adsorption of gases in multimolecular layers," *Journal of the American Chemical Society*, vol. 60, no. 2, pp. 309–319, 1938.

[37] K. S. Sing, "Reporting physisorption data for gas/solid systems with special reference to the determination of surface area and porosity (Recommendations 1984)," *Pure and Applied Chemistry*, vol. 57, no. 4, pp. 603–619, 1985.

[38] C. H. Giles, D. Smith, and A. Huitson, "A general treatment and classification of the solute adsorption isotherm. I. Theoretical," *Journal of Colloid And Interface Science*, vol. 47, no. 3, pp. 755–765, 1974.

[39] Y. Abe, K. Onisawa, S. Aratani, and M. Hanazono, "Temperature dependence in emission characteristics of an organic el cell with 8-hydroxyquinoline aluminum emitting layer," *Journal of the Electrochemical Society*, vol. 139, no. 3, pp. 641–643, 1992.

[40] G. P. Kushto, Y. Iizumi, J. Kido, and Z. H. Kafafi, "A matrix-isolation spectroscopic and theoretical investigation of tris(8-hydroxyquinolinato)aluminum(III) and tris(4-methyl-8-hydroxyquinolinato)aluminum(III)," *Journal of Physical Chemistry A*, vol. 104, no. 16, pp. 3670–3680, 2000.

New Pharmacophore from the Stem Bark Fractions of Acacia decurrens (Willd), an Invasive South Africa Tree

Bamidele Joseph Okoli and Johannes Sekomeng Modise
Institute of Chemical and Biotechnology, Vaal University of Technology, Southern Gauteng Science and Technology Park,
Private Bag X021, Vanderbijlpark, No. 1911, 5 Moshoeshoe Street, Sebokeng 1983, South Africa

INTRODUCTION

Invasive species are flora introduced into a foreign environment from their native host region and with significant consequences on the available resources in the host region [1].The chances of an invasive species establishing dominance ina new environment are minuscule, but research has proventhat once they do, the economic damage can be enormous[2]. Literature has shown that invasive species are responsiblefor threat on indigenous species, although some other biotic and abiotic factors might contribute [3].

Acacia (wattle) is native shrubs and trees to Australia, from the subfamily of Mimosoideae of the family Fabaceae,due to its prolific nature being found in all terrestrial habitats[4]. They are classified as a Category 2 invasive plant bythe Act on Alien and Invasive Species Regulations of SouthAfrica [5]; such exempted flora does require a permit to beintroduced to the environment [6].

Indigenous wildlife may not have the potentials of combating or competing against invasive species that has no predators on the food chain within the new environment[7]; however, this phytotolerance can be exploited for itspharmacological activity against infections of the region. Theplant parts have various applications in its native countryAustralia: the flowers are edible and the seed pods are usedfor the production of green dye, being grown for firewood oras a fast-growing windbreak or shelter tree.The gum from thetrunk is used as a low-quality gum arabic [8].

According to the report of Tewari and Jindal [9], O-Me derivatives of the dietary supplements, 2,3,4,6-tetra-O-methyl-D-galactose, 2,3-di-O-Methyl-L-arabinose, 2,3,4-tri-Omethyl-D-galactose, and 2,4-di-O-methyl-D-galactose, wereisolated from A. decurrens gum. Also, two novel diterpenoids,11,14,15-trihydroxy-12-methoxy-20-oxo-8,11,13-abietatrien-7-one and 10,11,14-trihydroxy-18-acetoxymethylene-12-me thoxy-8,11,13-abietatrien-7-one, with selective inhibitory activity against

MCF-7 and HT-29 cell lines, were isolated from the root extract of A. decurrens [10]. In addition tothe novel bioactive compounds isolated, the recent upsurgein pharmacological potentials for phytoantioxidants,phytoantimicrobial pharmacophore, and tolerance of A.decurrens for native invader has been a source of motivationfor the study of invasive vegetation as a source of thelead compound [8]. The selection of A. decurrens is notsolely dependent on ethnopharmacological knowledge ortraditional uses but by direct testing and bioassay-guidedisolation of compounds [11]. The generic protocol for thedrug discovery from natural products is employed in thestudy using bioassay-guided in vitro testing of the plantextracts and eventual isolation and identification of the bioactive compounds (see graphical abstract).

activity against MCF-7 and HT-29 cell lines, were isolated from the root extract of *A. decurrens* [10]. In addition to the novel bioactive compounds isolated, the recent upsurge in pharmacological potentials for phytoantioxidants, phytoantimicrobial pharmacophore, and tolerance of *A. decurrens* for native invader has been a source of motivation for the study of invasive vegetation as a source of the lead compound [8]. The selection of *A. decurrens* is not solely dependent on ethnopharmacological knowledge or traditional uses but by direct testing and bioassay-guided isolation of compounds [11]. The generic protocol for the drug discovery from natural products is employed in the study using bioassay-guided in vitro testing of the plant extracts and eventual isolation and identification of the bioactive compounds (see graphical abstract).

2. Experimental

2.1. Chemicals. The reagents and chemicals used in this study are from Sigma-Aldrich Chemicals Co., St. Louis, MO, USA, and are of analytical grade.

2.2. Collection and Extraction of A. decurrens Stem Bark. The fresh stem bark of *A. decurrens* was harvested around October 2016 near Vaal Dam Road, Heidelberg (26.5033°S, 28.4397°E), South Africa, diced, and dried at an ambient temperature at a relatively low humidity. Authentication of the of *A. decurrens* stem bark was carried out by the South Africa National Biodiversity Institute, Pretoria, and voucher specimen number: 1200-1, and was deposited at Pretoria National Botanical Garden. The extraction was performed by serial maceration using 4 L of each solvent: hexane, chloroform, ethyl acetate, and methanol with slight agitation at 111 revs/min for seven days. The solvents were removed using a rotary evaporator and the yield of the extracts was determined.

2.5. GC-MS Analysis of Compounds. The first step involves the solubilization of compounds AD1 and AD2 in chloroform and AD3 and AD4 in acetone prior to introduction into the GC injection port. The retention time and molecular ion determination were carried out on Clarus 500 PerkinElmer Gas Chromatograph equipped with an Elite-5 (100% dimethylpolysiloxane) column coupled to a mass spectrometer detector. The initial column temperature is set at 110°C and held for 2 min and the oven temperature increased at a rate of 5°C/min, to 230°C, and held for 9 min. The helium (He) flow rate was maintained at 1 ml/min, while keeping the injection port temperature at 250°C. The injection of the compounds was by split mode method of 10 : 1 with a mass scan range of 45–450 (m/z).

2.6. Spectroscopic Analysis of Compounds. Spectroscopic studies were carried out on the compounds by scanning the UV-Vis region using PerkinElmer Spectrophotometer and identification of functional groups by using VERTEX 80 FTIR Spectrophotometer and the 1D and 2D; the characterization was carried out on Agilent VnmrJ3 Spectrometer operating at 400 MHz.

2.7. Inoculums and Inoculation Procedure. Stock culture test organisms maintained at 4°C on slants of nutrient agar were obtained from the Biotechnology Department, Vaal University of Technology, South Africa. The growth method was employed in the standardisation of the inoculum density to achieve a concentration of 1.5×10^8 CFU/ml. The agar plates were cultured from colonies in a Mueller-Hinton broth and incubated at 37°C to 0.5 McFarland standard [18]. Furthermore, the inoculum suspension was used within a quarter of an hour to avoid any change in the size or loss of viability [19]. A uniform streaking of the dry Mueller-Hinton agar plate surface was conducted twice with standardised bacterial inoculum suspension.

2.3. Qualitative and Quantitative Phytochemical Screening. The fractions were analyzed for the presence of secondary metabolites using standard procedures. The total phenolic content (TPC) was determined, and the results were expressed in mg of gallic acid per g of the sample [12]. The total flavonoids (TFC) were measured and expressed as mg of rutin equivalents per g of the sample [13]. The tannin content (TC) measured and expressed as mg of tannin per g of the sample [14], and also the alkaloid, saponins, and terpenoids contents were determined and expressed in percentage [15–17].

2.4. Fractionation and Isolation of Compounds. The fractionation of the crude extracts was conducted on a Si-gel column of 640 mm by 60 mm with various solvent systems. The obtained bioactive fractions of the extracts were further subjected to subfractionation on a Si-gel column of 330 mm by 30 mm for isolation. Figure 1 is a summary of the fractionation, isolation, and purification of bioactive compounds from the extracts.

2.8. Preparation of Compound Impregnated Discs. Sensitivity discs of 6 mm diameter were immersed in stock solutions of each compound prepared by dissolving 50,000 μg of the compound in 5 ml of dimethyl sulfoxide [20]. The disc was sterilised by autoclaving at 121°C for 15 minutes and impregnated with 10 mg/ml of each compound. Dimethyl sulfoxide-loaded discs (negative controls), ampicillin (positive controls), and compound impregnated discs were dried in an incubator at 45°C for 24 h before the application on the bacterial lawn [21]. The disc diffusion method was carried out to investigate the in vitro sensitivity of *Micrococcus luteus* (ATCC 26883), *Staphylococcus aureus* (ATCC 25923), *Escherichia coli* (NCTC 11954), *Salmonella typhi* (ATCC 29692), *Klebsiella pneumonia* (BAA 1706), *Shigella sonnei* (ATCC 25931), *Staphylococcus epidermis* (ATCC 12228), *Listeria monocytogenes* (ATCC(R) BAA-751TM), and *Enterococcus faecalis* (ATCC 22735) against the compounds. The analysis was performed in triplicate.

2.9. Minimum Inhibitory Concentration (MIC). Microorganism sensitive compounds were screened to determine

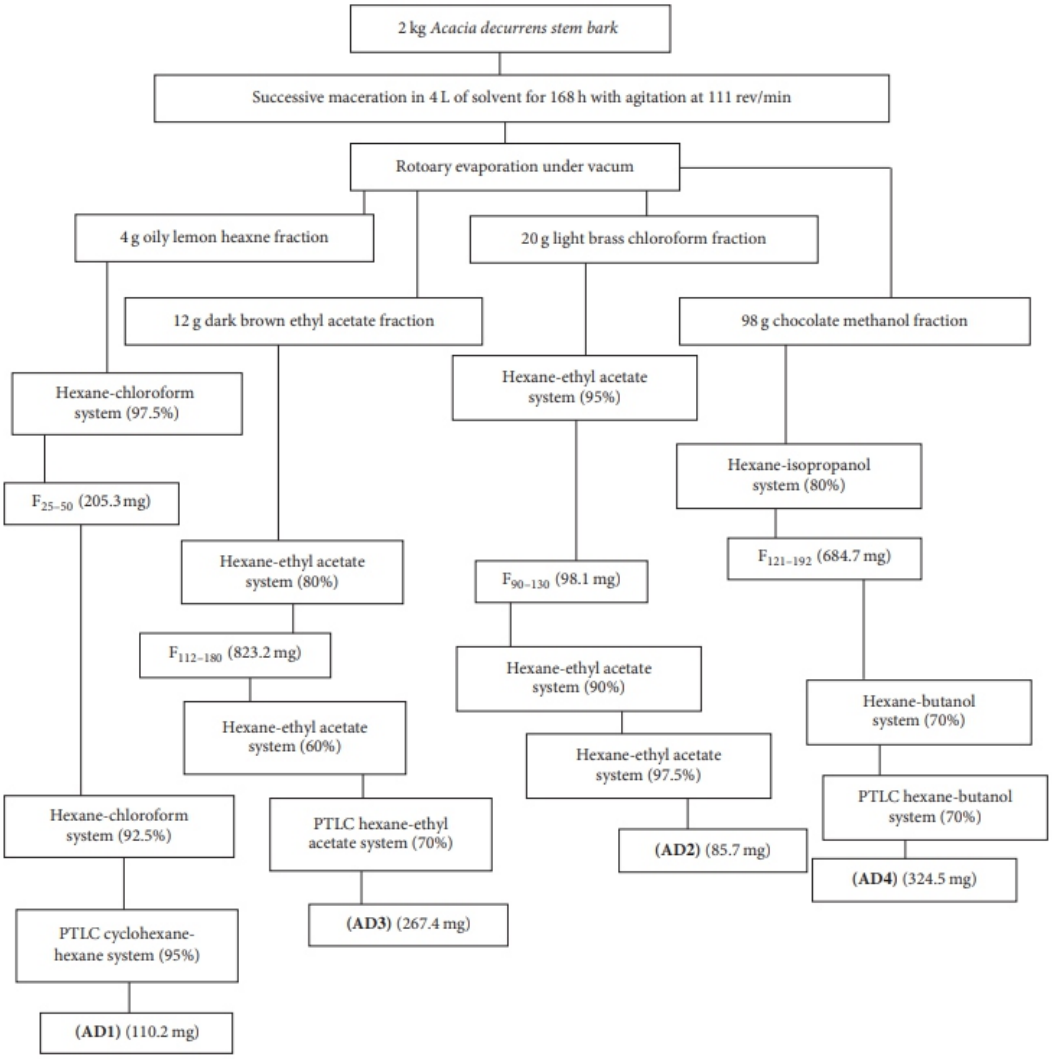

FIGURE 1: A brief summary of the general fractionation, isolation, and purification of bioactive compounds from the extracts.

the minimum inhibitory concentration by broth microdilution method [22]. The 12 wells of each row were filled with 0.5 ml sterilised Mueller-Hinton agar. To wells 3–12 sequentially, an additional 0.5 ml of a mixture of agar and compounds was serially diluted to create a concentration of 100–0.3906 μg/mL. The first well served as growth control and well 2 as an antibiotic control (ampicillin) with MIC of 3.125 μg/mL. The incubation of the deep wells was for 24 h at 37°C and turbidity was measured after 24 h at 600 nm using a PerkinElmer UV-Vis Spectrophotometer to determine the MIC. These tests were performed in triplicate.

2.10. DPPH Radical Scavenging Activity. The method of Blois with some modifications was applied to evaluate the ability of the compounds to scavenge the DPPH radicals [23]. Freshly prepared 300 μl of 0.05 mM methanolic solution of DPPH was added to 60 μl of 2-methyl-octahydro-indene-4-carboxylic acid (**AD**1), 6-methyldecahydro-1H-phenanthren-9-one (**AD**2), 8-hydroxytetradecahydro-chrysene-1-carbaldehyde (**AD**3), 8,9-dihydroxy-7-(2-hydroxy-ethyl)hexahydro-1H,3H-2-thia-5a-azacyclo penta[b]anthracen-6-one (**AD**4), ascorbic acid, and quercetin of different concentrations (50–250 μg/mL). Moreover, the mixture was vortexed and allowed for 30 min at 28°C in the absence of light. Then changes in the absorbance of the compounds were measured at 517 nm using a UV-Vis spectrophotometer. The comparative scavenging potentials of the compounds and standard antioxidants (quercetin and ascorbic acid) were expressed using the formula:

$$\% \text{ inhibition} = \frac{(A_B - A_A) \times 100}{A_B}, \quad (1)$$

where A_A and A_B are the absorbance of the test and blank, respectively. The IC_{50} (μM) was calculated using linear regression analysis. All analyses were carried out in triplicate.

2.11. Total Antioxidant Activity by ABTS$^{\bullet+}$ Decolourization Assay. In the method of Siddhuraju and Manian [24], the total antioxidant activity of the compounds was measured by the decolourization of ABTS$^{\bullet+}$. Exactly 7 mM of 2,2′-azinobis(3-ethylbenzothiazoline-6-sulfonic acid and 2.45 mM of potassium persulfate were prepared in distilled water, and the mixture was allowed to stand in the dark at ambient temperature for 24 h to generate the ABTS$^{\bullet+}$.

Table 1: Nature of the extracts and recovery yield/g of *A. decurrens* stem bark.

Menstruum	Physical nature	Colour	Recovery yield/g
Hexane	Oily	Lemon	0.21 ± 0.31
Chloroform	Solid	Light brass gold	1.20 ± 0.05
Ethyl acetate	Solid	Dark brown	0.63 ± 0.01
Methanol	Solid	Chocolate	4.72 ± 0.04

Table 2: Qualitative screening of the stem bark of *A. decurrens* of extracts.

Phytochemical	Fractions			
	Hexane	Chloroform	Ethyl acetate	Methanol
Alkaloids	+	++	–	–
Glycosides	+	+++	+++	+++
Phenols	–	+++	+++	++
Saponins	–	–	++	+++
Terpenoids	++	++	+++	+++
Tannins	++	+++	+++	+++
Flavonoids	–	–	+++	+++

–, absent; +, low in abundance; ++, moderate in abundance; +++, high in abundance.

and nature and the percentage yields were recorded. The methanolic fraction has a higher yield compared to the yield of chloroform, ethyl acetate, and hexane (Table 1).

This result implies that most of the secondary metabolites are hydrophilic in nature and consistent with the literature report which confirms methanol as the most suitable solvent for extraction of the polar secondary metabolite [25]. There has been a report that polarity significantly affects the recovery yields of the secondary metabolites from the plant [26].

3.2. Qualitative and Quantitative Phytochemical Screening. The phytochemical screening of the fractions reveals the presence of terpenoids, phenols, tannins, flavonoids, saponins, and alkaloids. All the menstruum contains terpenoids and tannins; however, the saponins were found only in the methanolic fraction (Table 2).

The methanolic and ethyl acetate fractions contain about 85.7% of the tested secondary metabolites with a high degree of precipitation, while hexane menstruum contains moderately 57.1%. The secondary metabolites identified have established pharmacological activities consequentially [27,

green $ABTS^{\bullet+}$ colour was produced. However, the ABTS cation radical solution was diluted with distilled H_2O to an absorbance of 1.00 at 734 nm. The 3 mL of the generated $ABTS^{\bullet+}$ solution was mixed with 30 μL of the compounds and Trolox (control). The antioxidant potential was expressed as the concentration of Trolox (μmol/g), having the equivalent antioxidant activity of the compounds on dry weight basis. The absorbance was read at 734 nm exactly after 30 min.

3. Results and Discussion

3.1. Influence of Menstruum on the Recovery Yield of Compounds. The fractions obtained were different in colours metabolites, other than growing invasive classification [29].

The alkaloid contents of the chloroform are higher than observed in hexane fraction (Figure 2(a)). However, the % steroids found in the hexane fraction is greater than chloroform, ethyl acetate, and methanol fractions (Figure 2(c)). High alkaloid and steroid contents in solvents of polarity index of 0.1–4.1 are an indication that they are primarily nonpolar, unlike the saponins which are richer in ethyl acetate compared to the methanol fraction (Figure 2(b)).

According to the literature, alkaloids, saponins, and steroids are potent antimicrobial compounds because of their ability to prevent the growth of a microorganism, activating

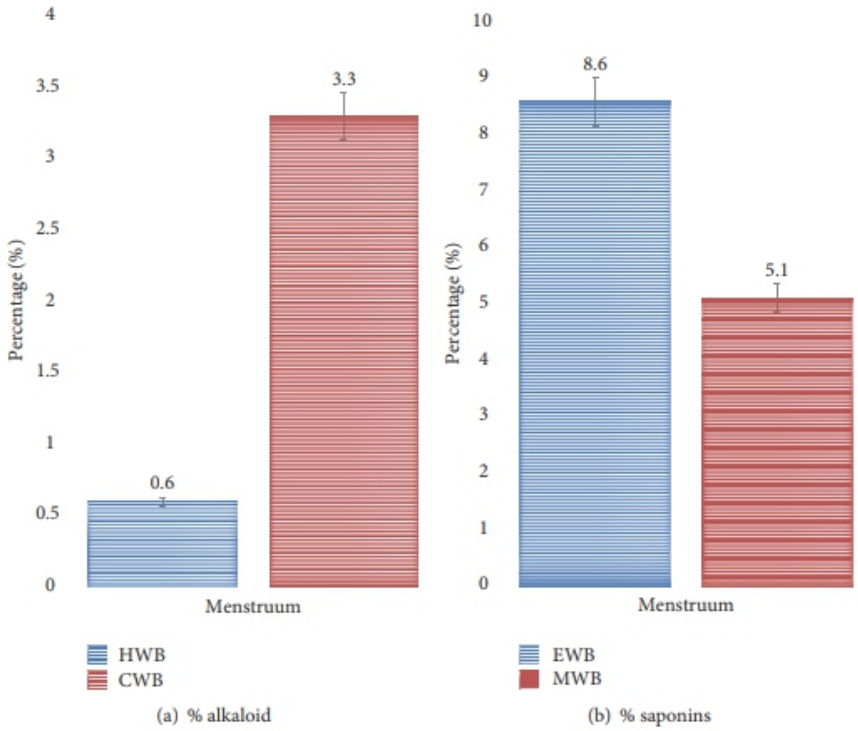

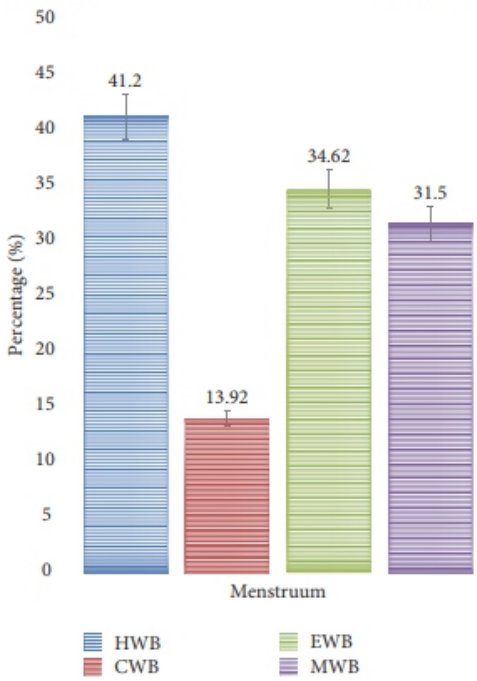

Figure 2: HWB: hexane wattle bark; CWB: chloroform wattle bark; EWB: ethyl acetate wattle bark; MWB: methanol wattle bark.

perturbations of the membrane [30] and interfering with gene expression pathways and metabolic processes [31].

The total phenolic contents of the chloroform fraction are higher than those observed in ethyl acetate and methanol fractions, calculated from the calibration curve (R^2 = 0.9903) (Figure 3(a)). The total flavonoid from the calibration curve (R^2 = 0.9986) is slightly higher in the methanol than ethyl acetate fraction (Figure 3(b)). However, the calibration curve

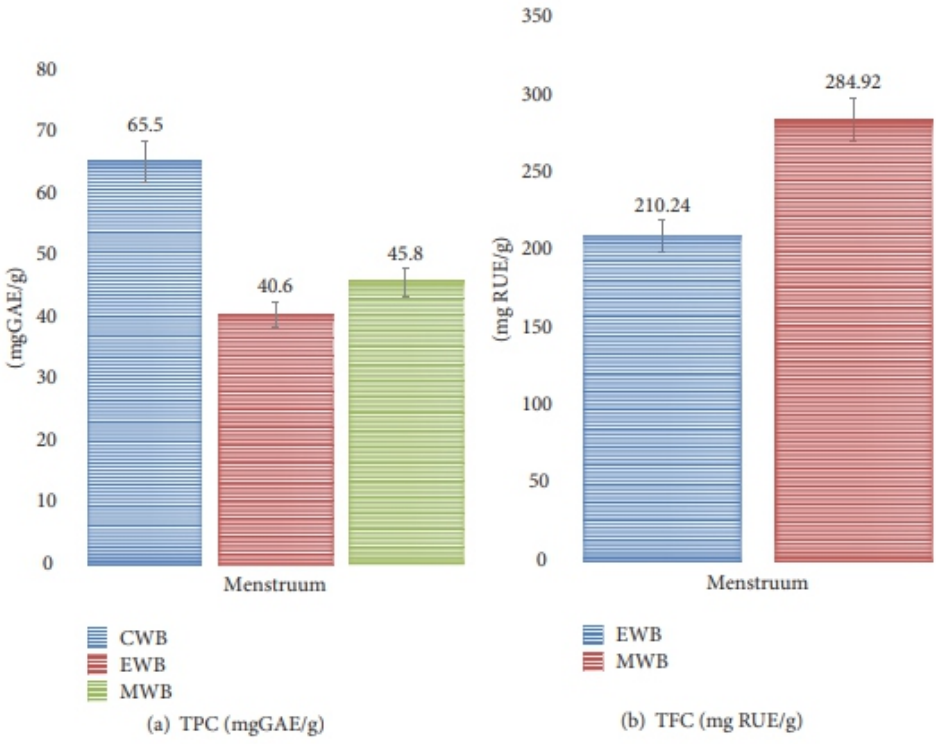

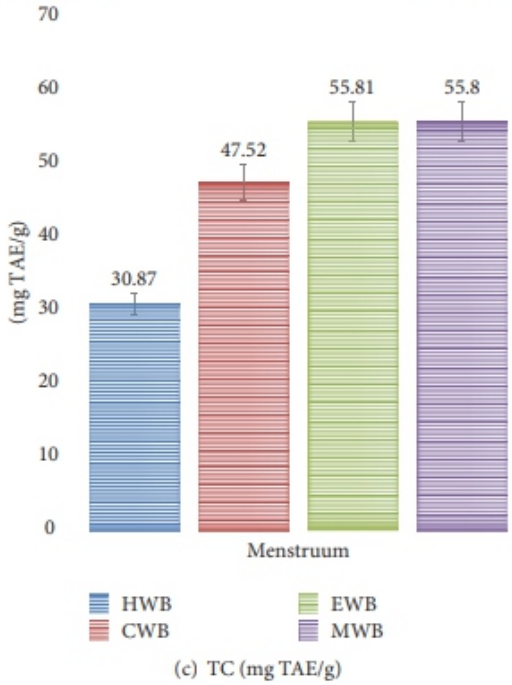

Figure 3: HWB: hexane wattle bark extract; CWB: chloroform wattle bark extract; EWB: ethyl acetate wattle bark extract; MWB: methanol wattle bark extract.

(R^2 = 0.9921) shows that the tannins are richer in solvents with polarity index 4.4–5.1, an indication of a highly polar class of tannins (Figure 3(c)). Reports have shown that phenols, flavonoids, and tannins have redox properties, which allow them to act as phytoantioxidants [32]. A significant rise in the level of the tannin and flavonoids extracted was observed as polarity changes with solvent. The observation above is because the tannins and flavonoids are water-soluble polyphenol class of compounds [33], and simple skeleton phenolic rings are connected by a propionic chain [34].

after purification (Rf: 0.84) with λmax 240 (ε 130) (see Supporting File 1, in Supplementary Material available online at https://doi.org/10.1155/2017/1815278). The retention time (see Supporting File 2) and molecular mass are 10.8 min and m/z 182 (see Supporting File 3), respectively.

The IR stretching vibration at 3293.87(s) cm^{-1} is an O-H of the carboxylic acid, and 2952.67(w) and 2843.39(w) are the sp^3 C-H of an alkane and C=O of a carboxylic acid at 1710.15(m). The sp^2 C-H bending vibrations of the alkane are at 1450.34(w) and 1410.80(w) cm^{-1}, and 1113.28(w) and 1014.66(w) cm^{-1} are the C-O stretching vibrations of carboxylic acid (see Supporting File 4).

^{1}H NMR δ_H (400 MHz, CD_3Cl) indicates carboxylic acid proton at 11.312 (1H, s, OH) ppm and methyl and methine protons at 2.15 (2H, m, 2-H), 1.74 (1H, m, 10-H), 1.40 (2H, m, 2-H), 1.41 (1H, m, 6-H), 1.24 (2H, m, 2-H), and 0.87 (3H, m, 11-H) ppm (see Supporting File 5).

^{13}C-NMR δ_c (400 MHz, CD_3Cl) indicates one methyl (CH_3) carbon at 19.68 (C-11) ppm, five methylene (CH_2) carbons at 32.74 (C-7), 30.04 (C-9), 29.38 (C-5), 26.89 (C-3), and 22.70 (C-4) ppm, four methine carbons at 37.09 (C-2), 31.93 (C-6), 30.87 (C-10), and 29.71 (C-8) ppm, and one quaternary carbon at 178.14 (C-1) ppm. Also observed is carboxylic acid carbon resonating at 178.14 (C-1) ppm, and a methine carbon at 37.09 (C-2) is attached to the carboxylic acid carbon (see Supporting File 6).

The HSQC spectrum shows a correlation between the protons at 2.15 (2H, m, 2-H) and 1.74 (1H, m, 10-H) and the methylene carbon at 32.74 (C-7) and 31.93 (C-6) ppm (see Supporting File 7). COSY data reveals a correlation between the protons at 2.15 (2H, m, 2-H) and 1.74 (1H, m, 10-H) ppm to the protons at 1.41 (1H, m, 6-H) and 1.24 (2H, m, 2-H) ppm (see Supporting File 8).

The HMBC shows that the proton at 11.312 (1H, s, OH) ppm is two bonds away from the carbon at 178.14 (C-1) ppm and three bonds away from the carbon at 37.09 ppm. Another notable correlation is between methine proton at 2.15 (2H,

*3.3. Characterization of 2-Methyl-octahydro-indene-4-carboxylic acid **(AD1)**.* 2-Methyl-octahydro-indene-4-carboxylic acid is obtained as a colourless oily compound (110.2 mg)

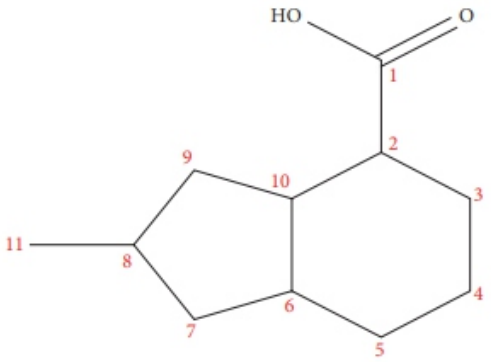

(AD1)

Scheme 1

CH_2), 1.23 (2H, m, CH_2), 1.08 (2H, d, CH_2), and methine proton at 1.71(1H, m, CH) and 1.46 (1H, m, CH) ppm (see Supporting File 12).

^{13}C-NMR δc (400 MHz, CD_3Cl) indicates the presence of fifteen carbon atoms with the carbon peaks resonating at 207.04 (C-1), 157.46 (C-7), 138.34 (C-2), 39.01 (C-14), 37.05 (C-6), 32.70 (C-4), 31.89 (C-8), 30.89 (C-5), 29.10 (C-13), 29.66 (C-12), 29.63 (C-9), 29.33 (C-10), 27.04 (C-11), 22.66 (C-3), and 19.67 (C-15) ppm (see Supporting File 13). ^{13}C-NMR reveals the presence of one methyl group at δc 19.67 (C-15), three methine carbons at δc 39.01 (C-14), 37.05 (C-6), and 32.70 (C-4) ppm, eight methylene carbons at δc 31.89 (C-8), 30.89 (C-5), 29.10 (C-13), 29.66 (C-12), 29.63 (C-9), 29.33 (C-10), 27.04 (C-11), and 22.66 (C-3) ppm, and three quaternary carbons at δc 207.04 (C-1), 157.46 (C-7), and 138.34 (C-2) ppm. The C=O stretching vibration of a ketone as observed in the FTIR spectrum at 1705.21 cm^{-1} is resonating at 207.04 (C-1) ppm; however, the peaks at 157.46 (C-7) and 138.34 (C-2) ppm are olefinic carbons corresponding to the stretching vibrational frequencies at 1640.01 and 1650.11 cm^{-1} on the FTIR spectrum (see Supporting File 11).

m, 2-H) ppm and the carbons at 30.87 (C-10) and 26.89 (C-3) ppm which are two bonds away (see Supporting File 9). The above spectroscopic data confirms structure as **AD1** (Scheme 1) with a molecular formula of $C_{11}H_{18}O_2$.

3.4. Characterization of 6-Methyldecahydro-1H-phenanthren-9-one ***(AD2)***. 6-Methyldecahydro-1H-phenanthren-9-one was isolated as a white wax (87.5 mg), melting point: 96–98°C, after purification (Rf: 0.81). The UV-Vis profile revealed peak at λmax 240 nm (ε 200) (see Supporting File 10).

The IR stretching vibrations at 2954.72(w), 2920.47(s), and 2851.24(s) are the sp^3 C-H of alkane, and C=O of a ketone at 1723(s), 1640(m), and 1650(m) is sp^2 C=C of an alkene. The bending vibrations of alkane sp^2 and sp^3 C-H are at 1462.67(m) cm^{-1} and 1377.32(m) cm^{-1}, respectively (see Supporting File 11).

^1H NMR δ_H (400 MHz, CD_3Cl) indicates 3.47 (2H, d, CH_2), 1.71 (1H, m, CH), 1.46 (1H, m, CH), 1.30 (2H, m, CH_2), 1.23 (2H, m, CH_2), 1.08 (2H, d, CH_2), and 0.92 (3H, d, CH_3) ppm. It establishes the presence of methyl at 0.92 (3H, d, CH_3) ppm, methylene protons at 3.47 (2H, d, CH_2), 1.30 (2H, m,

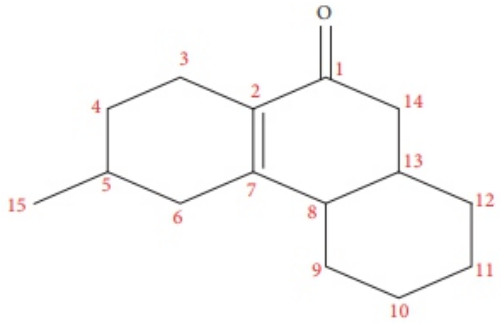

(AD2)

SCHEME 2

178–180°C, after purification: Rf: 0.68 with λ_{max} 240 nm (1.354) (see Supporting File 19). The retention time is 21.58 min (see Supporting File 20) and a molecular ion is at m/z 396 (see Supporting File 21).

The IR spectrum of 8-hydroxytetradecahydro-chrysene-1-carbaldehyde reveals the presence of -OH stretching vibration of alcohol at 3274 cm^{-1}, C-H of alkane 2968, 2945, 2919, and 2853 cm^{-1} the =C-H of aldehyde at 2869 cm^{-1}, C=O of aldehyde at 1735 cm^{-1}, and two peaks of C-O of alcohol at 1190 and 1097 cm^{-1}. The bending vibration at 1464 cm^{-1} is the C-H of alkane and 1386 cm^{-1} of C-H of alkane (see Supporting File 22).

^1H NMR δ_H (400 MHz, CD_3Cl) showed the presence of an aldehyde proton at 9.67 (1H, s, 26-H) ppm, two olefinic protons at 5.12 (1H, t, 12-H) and 5.20 (1H, d, 19-H) ppm,

The HSQC shows a correlation between the proton at δ 3.47 (2H, d, CH_2) ppm and the carbon peak at 39.01 (C-14) ppm (see Supporting File 14). The $^{1H\text{-}1H}$COSY spectrum shows that the methylene proton at 3.47 (2H, d, CH_2) and the methine proton at 1.71 (1H, m, CH) ppm are in the same chemical environment (see Supporting File 15).

The heteronuclear multiple bond correlation experiment reveals the correlations between carbons signals at 207.04 (C-1), 157.46 (C-7), and 138.34 (C-2) ppm and the proton at 3.47 (2H, d, CH_2) ppm (see Supporting File 16).

The GCMS analysis revealed a retention time of 15.98 min (see Supporting File 17) and a molecular ion peak at 218 (see Supporting File 18) which is in agreement with the molecular formula of $C_{15}H_{22}O$. The molecular structure of 6-methyldecahydro-1H-phenanthren-9-one based on the spectroscopic information above is deduced to be **AD2** (Scheme 2).

3.5. Characterization of 8-Hydroxytetradecahydro-chrysene-1-carbaldehyde ***(AD3)***. 8-Hydroxytetradecahydro-chrysene-1-carbaldehyde is a white needle (267.4 mg), melting point:

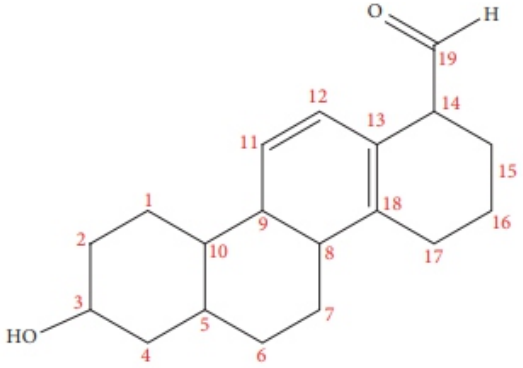

(AD3)

SCHEME 3

File 26). The aldehyde proton at 9.67 (1H, s, 26-H) ppm is three bonds away from the olefinic carbon peak at 145.18 (C-18) ppm. Also, the oxymethine proton peak at 3.20 (1H, m, 3-H) ppm shows correlation with 38.73 (C-10), 37.09 (C-8), and 27.14 (C-5) ppm methine protons and 18.34 (C-1) and 23.67 (C-15) methylene protons. The olefinic protons at 5.12 (1H, t, 12-H) and 5.20 (1H, d, 19-H) ppm show multiple bond correlations to carbon peaks at 25.97 (C-16) and 26.10 (C-6) ppm (see Supporting File 27). The structure and molecular formulas of 8-hydroxytetradecahydro-chrysene-1-carbaldehyde, inferred from the MS spectrum, 1 D NMR, COSY, and HMBC spectra, are confirmed as **AD3** (Scheme 3) and $C_{19}H_{42}O_2$, respectively.

oxymethine proton resonating at 3.20 (1H, m, 3-H) ppm, and hydroxyl proton at 1.59 (1H, s, OH) ppm (see Supporting File 23).

^{13}C NMR data δc (400 MHz, CD_3Cl) showed eight methine carbons at 38.73 (C-10), 37.09 (C-8), 31.07 (C-9), 27.14 (C-5), 55.11 (C-14), 78.96 (C-3), 120.13 (C-12), and 122.42 (C-11) ppm, eight methylene at 18.34 (C-1), 23.67 (C-15), 23.50 (C-7), 25.97 (C-16), 26.10 (C-6), 28.05 (C-17), 34.69 (C-2), and 47.58 (C-4) ppm, and three quaternary carbons at 186.36 (C-19), 140.00 (C-13), and 145.18 (C-18) ppm. The ^{13}C NMR spectrum revealed the presence of a carbonyl carbon at 186.36 (C-19) ppm, four olefinic carbon atoms resonating at 120.13 (C-12), 122.42 (C-11), 140.00 (C-13), and 145.18 (C-18) ppm, and an oxymethine carbon peak at 78.96 (C-3) ppm (see Supporting File 24).

The HSQC assignment of the proton at 9.67 (1H, s, 26-H) ppm to the carbonyl carbon at 186.36 (C-19) ppm is an indication that the proton is directly bonded. Also, the oxymethine proton at 3.20 (1H, m, 3-H) ppm shows correlation to carbon peak at 78.96 (C-3) ppm. The olefinic protons at 5.12 (1H, t, 12-H) and 5.20 (1H, d, 19-H) ppm show correlation to the carbon peaks at 120.13 (C-12) and 122.42 (C-11), respectively (see Supporting File 25).

The COSY spectrum indicates that the olefinic protons at 5.12 (1H, t, 12-H) and 5.20 (1H, d, 19-H) ppm show correlation to the methine protons at 1.98 and 1.94 ppm. There is a correlation between the oxymethine proton at 3.20 (1H, m, 3-H) ppm and the protons at 1.53 and 1.52 ppm (see Supporting

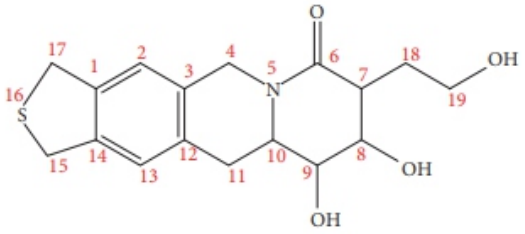

(AD4)

SCHEME 4

(C-13), 128.42 (C-2), 75.29 (C-9), 74.80 (C-8), 60.17 (C-19), 54.43 (C-10), 47.71 (C-4), 40.72 (C-17), 40.53 (C-15), 38.13 (C-7), 29.11 (C-11), and 27.79 (C-18) ppm.

The ^{1}H NMR spectrum revealed the presence of aromatic proton at 6.04 (1H, s, 2-H) and 6.04(1H, s, 13-H) ppm, oxy-methine proton resonating at 3.40 (2H, dd, 8-H) ppm, thiomethine protons resonating 3.70 (2H, s, 15-H) and 3.70 (2H, s, 17-H) ppm, and proton α to carbonyl at 1.96 (1H, m, 7-H) ppm (see Supporting File 32).

The ^{13}C-NMR spectrum showed seventeen carbon atoms of six methine (CH) carbons at 38.13 (C-7), 74.80 (C-8), 75.29 (C-9), 54.43 (C-10), 128.46 (C-13), and 128.42 (C-2) ppm, six methylene (CH_2) at 40.72 (C-17), 40.53 (C-15), 29.11 (C-11) 47.71 (C-4), 60.17 (C-19), and 27.79 (C-18) ppm, and six quaternary carbon atoms at 133.11 (C-1), 130.61 (C-3), 138.45 (C-12), 136.83 (C-14), and 176.72 (C-6) ppm. The ^{13}C NMR spectrum revealed the carbonyl carbon of an amide at 176.72 (C-6) ppm and the presence of six aromatic carbon atoms resonating at 138.45 (C-12), 136.83 (C-14), 133.11 (C-1), 130.61

3.6. Characterization of 8,9-Dihydroxy-7-(2-hydroxy-ethyl)-9, 9a-hexahydro-1H,3H-2-thia-5a-azacyclo penta[b]anthracen-6-one ***(AD4)***. 8,9-Dihydroxy-7-(2-hydroxy-ethyl)-9,9a-hexa-hydro-1H,3H-2-thia-5a-azacyclopenta[b]anthracen-6-one was isolated as a yellow semisolid (324.5 mg), melting point: 212–214°C, after purification Rf: 0.58 with a GC retention time of 23.25 mins (see Supporting File 28). The UV-Vis peak at λmax 240 nm (ε 1.333) (see Supporting File 29) and the mass spectrum revealed a molecular ion peak at m/z 333 (see Supporting File 30).

On the IR spectrum, an O-H stretching vibration of alcohol is observed at 3369.00(m) cm^{-1}, sp^3 C-H stretching vibration at 2924(m) cm^{-1}, S-C stretching vibration at 2498(m) cm^{-1}, and C=O stretching vibration of a tertiary amide at 1685(s). Also, bending vibrations were observed at the fingerprint region at 1019(s) cm^{-1} of C-O, aromatic C=C overtone at 1610(s) and 1407(m) cm^{-1}, and C-H aromatic bending vibrations at 985(s), 942(s), 929(s), 900(s), 837(s), and 758(s) cm^{-1} (see Supporting File 31).

^{1}H NMR δ_H (400 MHz, CD_3OD) indicated 6.04 (1H, s, 2-H), 6.04 (1H, s, 13-H), 3.98 (2H, s, 4-H), 3.77 (1H, m, 10-H), 3.73 (1H, dd, 9-H), 3.70 (2H, s, 15-H), 3.70 (2H, s, 17-H), 3.50 (2H, t, 19-H), 3.40 (2H, dd, 8-H), 2.32 (2H, d, 11-H), 1.96 (1H, m, 7-H), 1.86 (2H, m, 18-H), 1.84 (1H, s, 19-OH), 1.79 (1H, s, 8-OH), and 1.74 (1H, s, 9-OH) ppm.

^{13}C-NMR δc (400 MHz, Cd3OD) indicated 176.72 (C-6), 138.45 (C-12), 136.83 (C-14), 133.11 (C-1), 130.61 (C-3), 128.46

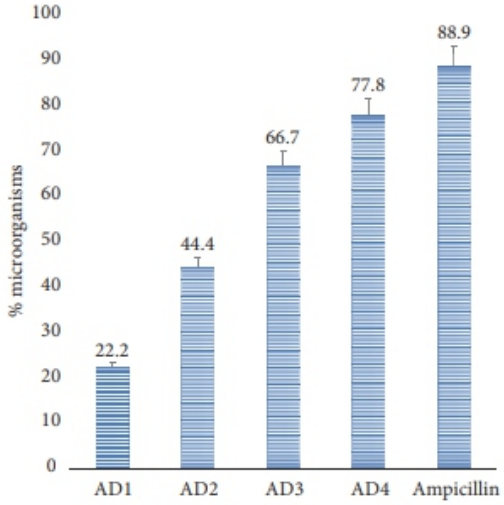

FIGURE 4: Antibacterial activity of the bioactive compounds.

strains, including six Gram-positive and three Gram-negative strains. The compounds **AD(1–4)** have little inhibitory activity against Gram-negative strains, but the results on the six Gram-positive strains were significant. Compounds **AD2, AD3,** and **AD4** were the most potent antimicrobial compounds inhibiting 44.4%, 66.7%, and 77.8% of the tested microorganisms, respectively (Table 3 and Figure 4). On the other hand, compound **AD1** has the lowest bacterial inhibition at 22.2% compared to the positive control and the other compounds.

(C-3), 128.46 (C-13), and 128.42 (C-2) ppm. Two oxymethine carbons peaked at 75.29 (C-9) and 74.80 (C-8) ppm and an oxymethylene peak appeared up field at 60.17 (C-19) ppm (see Supporting File 33).

The HSQC showed correlations between the aromatic carbons at 128.46 (C-13) and 128.42 (C-2) ppm and protons at 6.04 (1H, s, 2-H) and 6.04 (1H, s, 13-H) ppm. Also, there is a connection between the two oxymethine carbons at 75.29 (C-9) and 74.80 (C-8) ppm and the protons at 3.98 (2H, s, 4-H) and 3.77 (1H, m, 10-H) ppm (see Supporting File 34).

The COSY spectrum indicates that the aromatic protons at 6.04 (1H, s, 2-H) and 6.04(1H, s, 13-H) ppm are three bonds away from the thiomethylene protons at 3.73 (1H, dd, 9-H) and 3.70 (2H, s, 15-H) ppm (see Supporting File 35). The HMBCAD showed that the peaks at 176.72 (C-6), 138.45 (C-12), 136.83 (C-14), 133.11 (C-1), 130.61 (C-3), 128.46 (C-13), 128.42 (C-2), 74.80 (C-8), and 54.43 (C-10) ppm are close to the same chemical environment as the aromatic protons 6.04 (1H, s, 2-H) and 6.04 (1H, s, 13-H) ppm (see Supporting File 36 for full experimental data). The information from the 1D, HSQC, COSY, HMBCAD, and mass spectra of 8,9-dihydroxy-7-(2-hydroxy-ethyl)-9,9a-hexahydro-1H,3H-2-thia-5a-aza cyclopenta [b] anthracen-6-one confirms a structure of **AD4** (Scheme 4) and molecular formula $C_{18}H_{23}NO_3S$.

*3.7. Antimicrobial Potential of Compounds **AD1–AD4**.* The inhibition effect of the compounds is tested on nine bacterial

Compound **AD4** indicated the highest antimicrobial activity due to the presence of functional groups such as the thiol, hydroxyl, and amide. However, *E. coli* and *S. sonnei* were predominantly resistance, due to the production of β-lactamases as expected of Gram-negative organisms [35]; similar strength was observed for compounds AD2 and AD3.

For β-lactams to reach the binding proteins located in the inner membrane of the organism specific functional group is required. In this study, the bacterial cell production of β-lactamases was in insufficient concentration to tip the kinetics in favour of the destruction of compounds **AD2, AD3,** and **AD4**. Compound **AD1** clearly was ineffective due to the absence of the primary functional groups by decreasing penetration or actively extruding the antimicrobial compound [36]. The breaching of the intact cell walls and membranes of the peptidoglycan and cytoplasmic layer of *M. luteus, E. faecalis,* and *L. monocytogenes* is also due to the type of functional groups on compounds AD2, **AD3,** and **AD4**. They induce cells to lyse and cause breakage of walls and membranes. *M. luteus* and *L. monocytogenes* were sensitive to all tested compounds despite the fact that these organisms survive oligotrophic environments for extended periods of time [37], confirming the possible use of the compounds for the treatment of opportunistic infection caused by *M. luteus* and *L. monocytogenes* in immunosuppressed patients.

The MIC of bioactive compounds (Table 4) revealed that 8-hydroxytetradecahydro-chrysene-1-carbaldehyde **(AD3)** and 8,9-dihydroxy-7-(2-hydroxy-ethyl)-9,9a-hexahydro-1H,

Table 3: Sensitivity of the bioactive compounds against the test organisms.

Bacteria	(1)	(2)	(3)	(4)	Ampicillin
Staphylococcus aureus	−	−	−	+	+
Escherichia coli	−	−	−	−	−
Salmonella typhi	−	+	+	+	+
Klebsiella pneumoniae	−	−	−	+	+
Micrococcus luteus	+	+	+	+	+
Shigella sonnei	−	−	+	−	+
Staphylococcus epidermis	−	−	−	+	+
Listeria monocytogenes	+	+	+	+	+
Enterococcus faecalis	−	+	+	+	+

(+): susceptibility (inhibition zone ≥ 7 mm); (−): absence of susceptibility.

Table 4: Minimum inhibitory concentration (μg/ml) of the bioactive compounds.

Bacteria	(AD1)	(AD2)	(AD3)	(AD4)	Ampicillin
Staphylococcus aureus	—	—	12.5	12.5	12.5
Escherichia coli	—	—	—	—	—
Salmonella typhi	—	50	12.5	12.5	12.5
Klebsiella pneumoniae	—	—	—	—	6.25
Micrococcus luteus	50	50	12.5	12.5	6.25
Shigella sonnei	—	—	—	25	6.25
Staphylococcus epidermis	—	—	12.5	12.5	6.25
Listeria monocytogenes	50	50	12.5	6.25	6.25
Enterococcus faecalis	—	25	12.5	6.25	12.5

3H-2-thia-5a-azacyclopenta[b]anthracen-6-one **(AD4)** exhibited remarkable antibacterial activity toward the tested bacterial strains.

Compound **AD4** has a strong effect on *L. monocytogenes* and *E. faecalis* with MIC value of 6.25 μg/ml, whereas compounds **AD1** and **AD2** displayed destitute bacteriostatic activity with MIC value of 50 μg/ml. 8-Hydroxytetradecahydro-chrysene-1-carbaldehyde **(AD3)** also exhibited significant activity against *M. luteus, S. aureus, S. typhi, S. epidermis, L. monocytogenes,* and *E. faecalis* with MIC value of 12.5 μg/ml. However, only two compounds 8-hydroxytetradecahydro-chrysene-1-carbaldehyde **(AD3)** and 8,9-dihydroxy-7-(2-hydroxy-ethyl)-9,9a-hexahydro-1H,3H-2-thia-5a-azacyclopenta[b]anthracen-6-one **(AD4)** demonstrated strong anti-Gram-positive bacterial potential compared to ampicillin with MIC values ranging from 6.25 to 12.5 μg/ml. These results indicate that the stem bark of *A. decurrens* can be useful for the development of antibiotic and can also be a bioactive scaffold for new antibacterial drugs.

3.8. In Vitro Antioxidant Activity. The antioxidant capacity of compounds **AD(1–4)** was evaluation in vitro [38, 39], using DPPH a stable free radical acceptor of electron or hydrogen radical. Compounds **AD3** and **AD4** had significant scavenging effects on the DPPH radical, indicated by a colour (Table 5). As the concentration of 8-hydroxytetradecahydro-chrysene-1-carbaldehyde **(AD3)** and 8,9-dihydroxy-7-(2-hydroxy-ethyl)-9,9a-hexahydro-1H,3H-2-thia-5a-azacyclopenta[b]anthracen-6-one **(AD4)** increases from 50 to 250 μg/mL, so is the electrons taken up by DPPH radical. The radical scavenging strength of the compounds is in the order ascorbic acid > 8,9-dihydroxy-7-(2-hydroxy-ethyl)-9,9a-hexahydro-1H,3H-2-thia-5a-azacyclopenta[b]anthracen-6-one **(AD4)** > quercetin > 8-hydroxytetradecahydro-chrysene-1-carbaldehyde **(AD3)** > 2-methyl-octahydroindene-4-carboxylic acid **(AD2)** > 6-methyldecahydro-1H-phenanthren-9-one **(AD1)** with the IC_{50} (Table 5).

The study revealed that the 8-hydroxytetradecahydro-chrysene-1-carbaldehyde **(AD3)** and 8,9-dihydroxy-7-(2-hydroxy-ethyl)-9,9a-hexahydro-1H,3H-2-thia-5a-azacyclopenta[b]anthracen-6-one (AD4) were able to inhibit the potassium persulfate activity hence, reducing the production of $ABTS^{\bullet+}$ and exhibited higher ABTS radical scavenging activity. However, 2-methyl-octahydro-indene-4-carboxylic acid **(AD1)** and 6-methyldeca hydro-1H-phenanthren-9-one **(AD2)** are relatively weak antioxidant (Table 5).

The ascorbic acid used as a control in this study readily forms dehydroascorbate which does not possess radical scavenging potentials, but it easily reverts to ascorbate radical by donating an electron to the radical [40]. The radical anions on the oligonucleotides DNA are always prone to the attack of polyhydroxy compounds such as quercetin, and this explains the observed activities of compounds **AD4** and **AD3**. The comparable scavenging activity of compounds **AD4** due to the presence of the polyhydroxy groups in the neighbourhood of the aromatic ring is enhanced by the inductive effect of neighbouring groups, consequently, having the ease at which the protons are donated compared to

Table 5: Radical scavenging activity of the compounds from the stem bark of *A. decurrens*.

Compounds	DPPH radical scavenging activity IC_{50} values (μg/mL)	$ABTS^{\bullet+}$ scavenging activity (μmol of TE/g DW)
AD1	398.31 ± 0.21	1425.3 ± 167.2
AD2	439.29 ± 0.51	1945.9 ± 334.8
AD3	59.34 ± 0.07	3356.4 ± 253.7
AD4	30.07 ± 0.31	4363.2 ± 452.4
Ascorbic acid	15.75 ± 0.04	
Quercetin	45.74 ± 0.41	

quercetin and compounds **AD3**. 8-Hydroxytetradecahydro-chrysene-1-carbaldehyde **(AD3)** being a tetracyclic steroid has an equally likely activity due to the long carbon chains, imposing a lipophilic property which plays a significant role in the radical scavenging activity [41]. 2-Methyl-octahydro-indene-4-carboxylic acid **(AD1)** and 6-methyldecahydro-1H-phenanthren-9-one **(AD1)** are weak phytoantioxidant compounds due to the absence of electron donating and polyhydroxy groups on the structure.

4. Conclusion

The findings from this study confirm ethyl acetate and methanol as the most efficient solvent for extracting potent phytoantioxidant and antimicrobial metabolites. The generic protocol for the drug discovery from the *stem bark* of *A. decurrens* based on straightforward testing led to the isolation and identification of 2-methyl-octahydro-indene-4-carboxylic acid **(AD1)**, 6-methyldecahydro-1H-phenanthren-9-one **(AD2)**, 8-Hydroxytetradecahydro-chrysene-1-carb aldehyde **(AD3)**, and 8,9-dihydroxy-7-(2-hydroxy-ethyl)-9,9a-hexahydro-1H,3H-2-thia-5a-aza cyclo penta[b]anthracen-6-one **(AD4)**. 8-Hydroxytetradecahydro-chrysene-1-carbaldehyde and 8,9-dihydroxy-7-(2-hydroxy-ethyl)-9,9a-hexahydro-1H, 3H-2-thia-5a-azacyclopenta[b]anthracen-6-one have promising antimicrobial and antioxidant activity and could be new lead compounds. The free radical scavenging activity of 8,9-dihydroxy-7-(2-hydroxy-ethyl)-9,9a-hexahydro-1H,3H-2-thia-5a-azacyclopenta[b]anthracen-6-one **(AD4)** is comparatively stronger than quercetin. Further, immunological and toxicological studies must be carried out to establish the potential as a lead compound or the acetylated derivative tested in vivo to understand the biochemical interactions.

Additional Points

Supporting information including UV-Vis, GC-MS, and 1D and 2D NMR spectra of compounds AD(**1**–**4**) are available as supplementary material.

Conflicts of Interest

The authors declare no conflicts of interest.

Acknowledgments

The authors appreciate the Directorate of Research, Vaal University of Technology, and Northwest University, South Africa, for providing the facilities for the experiment.

References

[1] H. H. Kopelson, "The impacts of invasive plant species on human health," in *SUNY College of Environmental Science and Forestry Digital Commons @ ESF*, 2014, http://digitalcommons.esf.edu/citywild/6.

[2] M. H. Williamson, *doi.org/10.1016/j.crvi.2010.12.008*, Chapman and Hall, New York, NY, USA, 1996.

[3] L. J. Olson, "The economics of terrestrial invasive species: a review of the literature," *Agricultural and Resource Economics Review*, vol. 35, no. 1, pp. 178–194, 2006.

[4] U. Quattrocchi, *CRC World Dictionary of Grasses*, CRC Press, 2006.

[5] Department of Basic Education, "Government Gazette Staatskoerant," *Government Gazette*, vol. 583, no. 37230, pp. 1–4, 2014.

[6] B. Schreiner, "Water pricing: the case of South Africa," in *Water Pricing Experiences and Innovations*, A. Dinar, V. Pochat, and J. Albiac-Murillo, Eds., vol. 9 of *Global Issues in Water Policy*, pp. 289–311, Springer, Cham, 2015.

[7] W. J. Clinton, "Invasive Species," *Federal Register*, 1999, https://www.nwf.org/Wildlife/Threats-to-Wildlife/Invasive-Species.aspx.

[8] F. Pourmorad, S. J. Hosseinimehr, and N. Shahabimajd, "Antioxidant activity, phenol and flavonoid contents of some selected Iranian medicinal plants," *African Journal of Biotechnology*, vol. 5, no. 11, pp. 1142–1145, 2006.

[9] E. M. Anam, "Novel diterpenoids from acacia decurrens (Fabaceae)". Indian Journal of Chemistry Section B," *Indian Journal of Chemistry Section B, Organic Including Medicinal*, vol. 37, no. 12, pp. 1307–1309, 1998, https://eurekamag.com/research/003/215/003215125.php.

[10] A. Tewari and V. K. Jindal, "Studies on uronic acid materials and structure of Acacia decurrens gum polysaccharide," *Journal of Chemical and Pharmaceutical Research*, vol. 2, pp. 233–239, 2010, http://www.jocpr.com/.

[11] U. P. Albuquerque, P. M. de Medeiros, M. A. Ramos et al., "Are ethnopharmacological surveys useful for the discovery and development of drugs from medicinal plants?" *Brazilian Journal of Pharmacognosy*, vol. 24, no. 2, pp. 110–115, 2014.

[12] Q. V. Vuong, S. Hirun, P. D. Roach, M. C. Bowyer, P. A. Phillips, and C. J. Scarlett, "Effect of extraction conditions on total phenolic compounds and antioxidant activities of *Carica papaya* leaf aqueous extracts," *Journal of Herbal Medicine*, vol. 3, no. 3, pp. 104–111, 2013.

[13] J. Zhishen, T. Mengcheng, and W. Jianming, "The determination of flavonoid contents in mulberry and their scavenging effects on superoxide radicals," *Food Chemistry*, vol. 64, no. 4, pp. 555–559, 1999.

[14] R. Singh, P. Verma, and G. Singh, "Total phenolic, flavonoids and tannin contents in different extracts of artemisia absinthium," *Journal of Intercultural Ethnopharmacology*, vol. 1, no. 2, pp. 101–104, 2012.

[15] S. Fazel, M. Hamidreza, G. Rouhollah, and M. Verdian-Rizi, "Spectrophotometric determination of total alkaloids in some Iranian medicinal plants," *Journal of Applied Horticulture*, vol. 12, no. 1, pp. 69-70, 2010.

[16] H. P. Makkar, P. Siddhuraju, and K. Becker, "Methods in molecular biology: plant secondary metabolites," *Plant Secondary Metabolites*, vol. 393, pp. 47–49, 2007.

[17] H. Leffmann, "A text-book of pharmacognosy," *Journal of the Franklin Institute*, vol. 192, no. 5, pp. 690-691, 1921.

[18] J. H. Jorgensen and J. D. Turnidge, "Antibacterial susceptibility tests: dilution and disk diffusion methods," in *Manual of Clinical Microbiology*, pp. 1152–1172, ASM Press.11521172, Washington, DC, USA, 9th edition, 2007.

[19] C. O. Wilke, "Robustness and Evolvability in Living Systems," *BioScience*, vol. 56, no. 8, pp. 695-696, 2006.

[20] M. D. Mukhtar and A. Tukur, "Antimicrobial activity of extracts of pistia strtatiotes L," *Journal of the Nigerian Society for Experimental Biology*, vol. 1, no. 1, pp. 51–60, 2000.

[21] M. R. S. Zaidan, A. Noor Rain, A. R. Badrul, A. Adlin, A. Norazah, and I. Zakiah, "In vitro screening of five local medicinal plants for antibacterial activity using disc diffusion method," *Tropical Biomedicine*, vol. 22, no. 2, pp. 165–170, 2005.

[22] I. Wiegand, K. Hilpert, and R. E. W. Hancock, "Agar and broth dilution methods to determine the minimal inhibitory concentration (MIC) of antimicrobial substances," *Nature Protocols*, vol. 3, no. 2, pp. 163–175, 2008.

[23] M. S. Blois, "Antioxidant determinations by the use of a stable free radical," *Nature*, vol. 181, no. 4617, pp. 1199-1200, 1958.

[24] P. Siddhuraju and S. Manian, "The antioxidant activity and free radical-scavenging capacity of dietary phenolic extracts from horse gram (Macrotyloma uniflorum (Lam.) Verdc.) seeds," *Food Chemistry*, vol. 105, no. 3, pp. 950–958, 2007.

[25] M. Bhebhe, T. N. Füller, B. Chipurura, and M. Muchuweti, "Effect of solvent type on total phenolic content and free radical scavenging activity of black tea and herbal infusions," *Food Analytical Methods*, vol. 9, no. 4, pp. 1060–1067, 2016.

[26] T. Dhanani, S. Shah, N. A. Gajbhiye, and S. Kumar, "Effect of extraction methods on yield, phytochemical constituents and antioxidant activity of Withania somnifera," *Arabian Journal of Chemistry*, vol. 10, no. 1, pp. S1193–S1199, 2013.

[27] I. C. W. Arts and P. C. H. Hollman, "Polyphenols and disease risk in epidemiologic studies 1–4," *American Journal of Clinical Nutrition*, vol. 81, pp. 317–325, 2005.

[28] B. Manjunatha, "Antibacterial activity of Pterocarpus santalinus," *Indian Journal of Pharmaceutical Sciences*, vol. 68, no. 1, pp. 115-116, 2006.

[29] W. R. Elliot and D. L. Jones, *Encyclopaedia of Australian plants suitable for cultivation*, Lothian Press, Port Melbourne, Australia, 2nd edition, 2002.

[30] A. H. M. M. Rahman, "Traditional medicinal plants used in the treatment of different skin diseases of santals at abdullahpur village under akkelpur upazilla of joypurhat district , Bangladesh," *Gloss. Indian Med. Plants*, vol. 1, no. 2, pp. 17–20, 2013.

[31] G. C. Omojate, F. O. Enwa, A. O. Jewo, and C. O. Eze, "Mechanisms of Antimicrobial Actions of Phytochemicals against Enteric Pathogens A—Review," *J. Pharm. Chem. Biol. Sci*, vol. 2, no. 2, pp. 77–85, 2014.

[32] M. A. Soobrattee, V. S. Neergheen, A. Luximon-Ramma, O. I. Aruoma, and T. Bahorun, "Phenolics as potential antioxidant therapeutic agents: Mechanism and actions," *Mutation Research—Fundamental and Molecular Mechanisms of Mutagenesis*, vol. 579, no. 1-2, pp. 200–213, 2005.

[33] C. M. Simões and E. P. Schenkel, "A pesquisa e a produção brasileira de medicamentos a partir de plantas medicinais: a necessária interação da indústria com a academia," *Revista Brasileira de Farmacognosia*, vol. 12, no. 1, pp. 35–40, 2002.

[34] W. C. Dornas, T. T. Oliveira, R. G. Rodrigues-das-Dores, A. F. Santos, and T. J. Nagem, "Flavonóides: potencial terapêutico no estresse oxidativo," *Revista de Ciências Farmacêuticas Básica e Aplicada*, vol. 28, no. 31, pp. 241–249, 2007.

[35] K. Bush, "The ABCD's of β-lactamase nomenclature," *Journal of Infection and Chemotherapy*, vol. 19, no. 4, pp. 549–559, 2013.

[36] K. Bush and G. A. Jacoby, "Updated functional classification of beta-lactamases," *Antimicrobial Agents and Chemotherapy*, vol. 54, no. 3, pp. 969–976, 2010.

[37] C. L. Greenblatt, J. Baum, B. Y. Klein, S. Nachshon, V. Koltunov, and R. J. Cano, "Micrococcus luteus - Survival in amber," *Microbial Ecology*, vol. 48, no. 1, pp. 120–127, 2004.

[38] C. G. Ramos, S. A. Sousa, A. M. Grilo, J. R. Feliciano, and J. H. Leitão, "The second RNA chaperone, Hfq2, is also required for survival under stress and full virulence of Burkholderia cenocepacia J2315," *Journal of Bacteriology*, vol. 193, no. 7, pp. 1515–1526, 2011.

[39] C. W. Choi, S. C. Kim, S. S. Hwang et al., "Antioxidant activity and free radical scavenging capacity between Korean medicinal plants and flavonoids by assay-guided comparison," *Plant Science*, vol. 163, no. 6, pp. 1161–1168, 2002.

[40] S. B. Nimse and D. Pal, "Free radicals, natural antioxidants, and their reaction mechanisms," *RSC Advances*, vol. 5, no. 35, pp. 27986–28006, 2015.

[41] V. Krishnamachari, L. H. Levine, and P. W. Paré, "Flavonoid oxidation by the radical generator AIBN: a unified mechanism for quercetin radical scavenging," *Journal of Agricultural and Food Chemistry*, vol. 50, no. 15, pp. 4357–4363, 2002.

Instructions for Authors

Essentials for Publishing in this Journal

1 Submitted articles should not have been previously published or be currently under consideration for publication elsewhere.

2 Conference papers may only be submitted if the paper has been completely re-written (taken to mean more than 50%) and the author has cleared any necessary permission with the copyright owner if it has been previously copyrighted.

3 All our articles are refereed through a double-blind process.

4 All authors must declare they have read and agreed to the content of the submitted article and must sign a declaration correspond to the originality of the article.

Submission Process

All articles for this journal must be submitted using our online submissions system. http://enrichedpub.com/ . Please use the Submit Your Article link in the Author Service area.

Manuscript Guidelines

The instructions to authors about the article preparation for publication in the Manuscripts are submitted online, through the e-Ur (Electronic editing) system, developed by **Enriched Publications Pvt. Ltd**. The article should contain the abstract with keywords, introduction, body, conclusion, references and the summary in English language (without heading and subheading enumeration). The article length should not exceed 16 pages of A4 paper format.

Title

The title should be informative. It is in both Journal's and author's best interest to use terms suitable. For indexing and word search. If there are no such terms in the title, the author is strongly advised to add a subtitle. The title should be given in English as well. The titles precede the abstract and the summary in an appropriate language.

Letterhead Title

The letterhead title is given at a top of each page for easier identification of article copies in an Electronic form in particular. It contains the author's surname and first name initial .article title, journal title and collation (year, volume, and issue, first and last page). The journal and article titles can be given in a shortened form.

Author's Name

Full name(s) of author(s) should be used. It is advisable to give the middle initial. Names are given in their original form.

Contact Details

The postal address or the e-mail address of the author (usually of the first one if there are more Authors) is given in the footnote at the bottom of the first page.

Type of Articles

Classification of articles is a duty of the editorial staff and is of special importance. Referees and the members of the editorial staff, or section editors, can propose a category, but the editor-in-chief has the sole responsibility for their classification. Journal articles are classified as follows:

Scientific articles:

1. Original scientific paper (giving the previously unpublished results of the author's own research based on management methods).

2. Survey paper (giving an original, detailed and critical view of a research problem or an area to which the author has made a contribution visible through his self-citation);

3. Short or preliminary communication (original management paper of full format but of a smaller extent or of a preliminary character);

4. Scientific critique or forum (discussion on a particular scientific topic, based exclusively on management argumentation) and commentaries. Exceptionally, in particular areas, a scientific paper in the Journal can be in a form of a monograph or a critical edition of scientific data (historical, archival, lexicographic, bibliographic, data survey, etc.) which were unknown or hardly accessible for scientific research.

Professional articles:

1. Professional paper (contribution offering experience useful for improvement of professional practice but not necessarily based on scientific methods);
2. Informative contribution (editorial, commentary, etc.);
3. Review (of a book, software, case study, scientific event, etc.)

Language

The article should be in English. The grammar and style of the article should be of good quality. The systematized text should be without abbreviations (except standard ones). All measurements must be in SI units. The sequence of formulae is denoted in Arabic numerals in parentheses on the right-hand side.

Abstract and Summary

An abstract is a concise informative presentation of the article content for fast and accurate Evaluation of its relevance. It is both in the Editorial Office's and the author's best interest for an abstract to contain terms often used for indexing and article search. The abstract describes the purpose of the study and the methods, outlines the findings and state the conclusions. A 100- to 250-Word abstract should be placed between the title and the keywords with the body text to follow. Besides an abstract are advised to have a summary in English, at the end of the article, after the Reference list. The summary should be structured and long up to 1/10 of the article length (it is more extensive than the abstract).

Keywords

Keywords are terms or phrases showing adequately the article content for indexing and search purposes. They should be allocated heaving in mind widely accepted international sources (index, dictionary or thesaurus), such as the Web of Science keyword list for science in general. The higher their usage frequency is the better. Up to 10 keywords immediately follow the abstract and the summary, in respective languages.

Acknowledgements

The name and the number of the project or programmed within which the article was realized is given in a separate note at the bottom of the first page together with the name of the institution which financially supported the project or programmed.

Tables and Illustrations

All the captions should be in the original language as well as in English, together with the texts in illustrations if possible. Tables are typed in the same style as the text and are denoted by numerals at the top. Photographs and drawings, placed appropriately in the text, should be clear, precise and suitable for reproduction. Drawings should be created in Word or Corel.

Citation in the Text

Citation in the text must be uniform. When citing references in the text, use the reference number set in square brackets from the Reference list at the end of the article.

Footnotes

Footnotes are given at the bottom of the page with the text they refer to. They can contain less relevant details, additional explanations or used sources (e.g. scientific material, manuals). They cannot replace the cited literature.
The article should be accompanied with a cover letter with the information about the author(s): surname, middle initial, first name, and citizen personal number, rank, title, e-mail address, and affiliation address, home address including municipality, phone number in the office and at home (or a mobile phone number). The cover letter should state the type of the article and tell which illustrations are original and which are not.

Notes: